



**HAL**  
open science

## Inter-laboratory comparison of discharge measurements with Acoustic Doppler Current Profilers, Chauvan field experiments, 8, 9 and 10th November 2016, Preliminary report

A. Despax, A. Hauet, Jérôme Le Coz, Guillaume Dramais, B. Blanquart, D. Besson, A. Belleville

### ► To cite this version:

A. Despax, A. Hauet, Jérôme Le Coz, Guillaume Dramais, B. Blanquart, et al.. Inter-laboratory comparison of discharge measurements with Acoustic Doppler Current Profilers, Chauvan field experiments, 8, 9 and 10th November 2016, Preliminary report. [Research Report] irstea. 2017, pp.92. hal-02606345

**HAL Id: hal-02606345**

**<https://hal.inrae.fr/hal-02606345>**

Submitted on 16 May 2020

**HAL** is a multi-disciplinary open access archive for the deposit and dissemination of scientific research documents, whether they are published or not. The documents may come from teaching and research institutions in France or abroad, or from public or private research centers.

L'archive ouverte pluridisciplinaire **HAL**, est destinée au dépôt et à la diffusion de documents scientifiques de niveau recherche, publiés ou non, émanant des établissements d'enseignement et de recherche français ou étrangers, des laboratoires publics ou privés.



# Inter-laboratory comparison of discharge measurements with Acoustic Doppler Current Profilers

Chauvan field experiments  
8, 9 and 10th November 2016

Preliminary report







*Preliminary version, February 13, 2017*

*Authors:*

AURÉLIEN DESPAX<sup>1</sup>, ALEXANDRE HAUET<sup>2</sup>, JÉRÔME LE COZ<sup>1</sup>, GUILLAUME DRAMAIS<sup>1</sup>, BERTRAND BLANQUART<sup>3</sup>, DAVID BESSON<sup>4</sup>, ARNAUD BELLEVILLE<sup>2</sup>.

*Affiliations:*

<sup>1</sup> Irstea, UR HHLY, 5 rue de la Doua, 69100 Villeurbanne, France, mail : aurelien.despax@irstea.fr

<sup>2</sup> EDF-DTG, 21 Avenue de l'Europe, BP 41, 38040 Grenoble, France

<sup>3</sup> Conseil et formation en métrologie, 40 Avenue du Général Leclerc, 54600 Villers les Nancy, France

<sup>4</sup> DREAL Centre Val de Loire, 5, avenue Buffon, 45064 Orléans, France

*Pictures (Source: A. Despax): front cover (top to bottom): ADCP measurements downstream of Chauvan dam and Q-liner upstream of EDF-DTG hydrometric station ; opening chapter pictures.*





## Contents

<b>1</b>	<b>Introduction and objectives</b> .....	<b>1</b>
1.1	Review of inter-laboratory experiments	1
1.2	Objectives	2
<b>2</b>	<b>The experimental design</b> .....	<b>3</b>
2.1	Participants	3
2.2	Equipment	4
2.2.1	ADCPs and tethered boats .....	4
2.2.2	Software .....	5
2.3	Logistics	6
2.3.1	Schedule .....	6
2.3.2	International hydrometry workshop .....	6
2.3.3	Safety .....	7
2.4	Site presentation	7
2.4.1	Cross-sections .....	7
2.5	Evaluation of the cross-section quality	9
2.5.1	By teams .....	9
2.5.2	By cross-sections .....	10
2.6	Measurements	11
2.6.1	Hydraulic conditions .....	11
2.6.2	Water-level monitoring and additional measurements .....	12
2.6.3	Measurement sessions - experimental plan .....	13

<b>3</b>	<b>Results</b>	<b>15</b>
3.1	Stage time series	15
3.2	Flow steadiness	16
3.3	Independent discharge measurements	19
3.3.1	Dye dilution gaugings	19
3.3.2	Section by section ADCP measurements	19
3.3.3	Continuous ADCP measurements	19
3.4	Summary of discharge estimates	19
3.5	ADCP measurement results	20
3.5.1	Results for each session	20
3.5.2	Results for each team	21
3.5.3	Results for each cross-section	21
3.6	Corrected discharge estimates	24
3.6.1	Corrected discharge values by team	24
3.6.2	Corrected discharge values by cross-section	24
3.6.3	Measured discharge ratio by cross-section	25
<b>4</b>	<b>Preliminary analysis</b>	<b>27</b>
4.1	Statistical analysis	27
4.1.1	Dispersion of results for each team	27
4.1.2	Dispersion and deviation by cross-section	28
4.2	Subjective analysis versus objective analysis	29
4.3	Uncertainty based on inter-laboratory experiments	30
4.3.1	Results based on corrected discharge estimates	31
4.3.2	Uncertainty estimates according to ADCP models (M9 versus StreamPro)	31
<b>5</b>	<b>Conclusions and perspectives</b>	<b>33</b>
	<b>Appendix</b>	<b>35</b>
<b>A</b>	<b>Bonus</b>	<b>35</b>
<b>B</b>	<b>Teams</b>	<b>39</b>
<b>C</b>	<b>Cross-sections</b>	<b>53</b>
C.1	Upstream-downstream views	53
C.2	Cross-section characteristics	59

---

<b>D</b>	<b>Procedure</b> .....	<b>61</b>
D.1	Incident sheets	61
D.2	Road map	62
<b>E</b>	<b>Rating-curve gaugings</b> .....	<b>63</b>
<b>F</b>	<b>Dye dilution report</b> .....	<b>65</b>
<b>G</b>	<b>Principles and computations for estimating uncertainty</b> .....	<b>67</b>
G.1	Processing of the comparison results	68
G.2	Estimation of the streamgauging technique bias	69
G.3	Uncertainty of the uncertainty estimates	70
G.4	Averaged discharge measurements	71
	<b>Bibliography</b> .....	<b>73</b>





A photograph of a river with a boat and trees. The river is dark and calm, with a small boat in the middle ground. The background is a dense forest of trees with green and yellow leaves. A white rope is visible in the foreground, extending from the left side towards the boat. A semi-transparent teal banner with rounded ends is overlaid on the bottom part of the image, containing the word "Disclaimer" in black text.

## Disclaimer

**This document is a preliminary report. Data come from measurement values directly given by operators.**

**Results presented here are deliberately restricted to a brief analysis. Additional work will be conducted after post-processing data using QRev software, in cooperation with the USGS (F. Engel and K. Oberg).**





## Résumé

Du 8 au 10 novembre 2016, le Groupe Doppler Hydrométrie a organisé sur le Taurion, à l'aval du barrage-usine de Chauvan, une campagne d'essais interlaboratoires de mesures de débit par profileur hydro-acoustique ADCP. En plus de permettre aux équipes participantes de confronter leurs outils et leurs pratiques, les essais interlaboratoires visent à contribuer collectivement à l'amélioration de la maîtrise de ces mesures et de leurs incertitudes. En l'absence de mesure de référence en termes de débit, les intercomparaisons constituent en effet un moyen utile pour quantifier l'incertitude de la technique de mesure dans des conditions de mesure données (Blanquart, 2013; Dramais *et al.*, 2013; Le Coz *et al.*, 2016).

Cette 5<sup>ème</sup> campagne interlaboratoire du Groupe Doppler Hydrométrie (après celles de la Vézère en 2009, de Génissiat en 2010 et 2012 ainsi que celle du canal de la Gentille en 2011) a rassemblé 50 participants (ou équipes de mesure) français et étrangers issus d'organismes publics ou privés, permettant la réalisation de plus de 600 mesures de débit réparties sur 3 demi-journées en profitant de débits stables délivrés par le barrage-usine de Chauvan, de l'ordre de  $14 \text{ m}^3/\text{s}$ .

Les essais interlaboratoires de Chauvan se distinguent par leur dimension et par l'originalité du protocole d'essai mis en œuvre.

Alors que les campagnes précédentes ont eu lieu sur des sites de mesure plutôt favorables, caractérisés par des géométries de section en travers relativement simples, des sections de mesure plus variées et complexes ont cette fois été choisies (faibles profondeurs, écoulements parfois perturbés par des obstacles). Ainsi des permutations ont été réalisées par 48 participants parmi les 24 sections de mesure présentant des conditions de déploiement plus ou moins favorables pour les ADCP.

En parallèle, le débit a été mesuré en continu par deux ADCP (StreamPro et Q-Liner) sur des sections de mesure fixes et les hauteurs d'eau ont été enregistrées par trois capteurs limnimétriques (deux sondes piézométriques relatives (Paratronic) disposées sur deux sections de mesure et un radar (VEGA) au niveau de la station hydrométrique EDF-DTG).

Le suivi limnimétrique a permis de confirmer la stabilité du débit du cours d'eau (variations inférieures à  $\pm 1$  cm) au cours des trois sessions de mesure. Les résultats de débit des ADCP sont peu dispersés (écarts-types de l'ordre de  $0,400 \text{ m}^3/\text{s}$ ) et la valeur de débit moyenne (référence construite) est proche des valeurs fournies par les mesures indépendantes à moins de 5% près (jaugeages par ADCP en continu aux deux sections fixes, jaugeage par la méthode globale de dilution et débit associé à la courbe de tarage selon la méthode de tracé conventionnelle, selon la méthode GesDyn ou selon la méthode BaRatin).

Les premiers résultats montrent que la dispersion des valeurs de débit semble nettement corrélée à la qualité des sections de mesure évaluée *in situ* par les équipes de mesure ainsi qu'au ratio du débit mesuré.

Les essais interlaboratoires conduisent à une évaluation d'incertitude de l'ordre de  $\pm 6\%$  (au niveau de confiance de 95 %, soit un facteur d'élargissement  $k=2$ ) pour un jaugeage par ADCP comportant 6 transects de mesure (dans les conditions de l'essai). Le nombre important de participants rassemblés permet une évaluation précise de cette incertitude de mesure bien que l'estimation de l'incertitude liée au biais de la technique de mesure reste problématique. Cette estimation reste néanmoins à affiner après homogénéisation des traitements des mesures à l'aide du logiciel QRev (Mueller, 2016).

La permutation des équipes au sein des différentes sections de mesure permettra la conduite d'une étude statistique visant à isoler l'incertitude liée à la section de mesure. Les résultats préliminaires tendent à montrer l'utilité de mesurer le débit sur plusieurs sections de mesure afin de réduire l'incertitude sur l'estimation du débit.

Enfin nous prévoyons de comparer les estimations d'incertitude par propagation des incertitudes telles que proposées par les logiciels Oursin (CNR), QRev (USGS), RiverFlowUA (South Florida Water management District), QMSys ou encore QUANT (Water Survey of Canada) aux résultats d'incertitude issus de ces essais interlaboratoires.

The image shows a wide river with dark, rippling water. In the foreground, a long, thin black pole extends from the top right towards the center of the river. At the end of the pole, there is a small orange boat or platform with a blue cylindrical object on it. The background shows a forested bank with trees in autumn colors. A semi-transparent teal banner with rounded corners is overlaid on the bottom part of the image, containing the word 'Abstract' in white text.

## Abstract


Quantifying the uncertainty of discharge measurements (or “gaugings”) is a challenge in the hydro-metric community. A useful tool to empirically estimate the uncertainty of a gauging method is the field inter-laboratory experiment (Le Coz et al., 2016). Previous inter-laboratory experiments conducted in France (in 2009, 2010 and 2012) showed that the expanded uncertainty of an ADCP gauging (considering an average discharge over six successive transects) is typically around 5% (with a probability level of 95%), under optimum measurement conditions (straight reach, uniform and smooth streambed cross-section, homogeneous flow, etc.). In practice, the selected cross-section does not always match all quality requirements which may result in larger uncertainty. However, the uncertainty due to site selection is very difficult to estimate with predictive equations.

From 8 to 10 November 2016, 50 laboratories or teams (from 8 different countries) with 50 ADCPs, simultaneously conducted more than 600 ADCP discharge measurements in steady flow conditions (around  $14 \text{ m}^3/\text{s}$  released by a dam), during three half-days, over 500 m along the Taurion River at Saint-Priest-de-Taurion, France. 26 cross-sections with various shapes and flow conditions, and more or less favourable conditions, were distributed along the river. A specific experiment procedure, which consisted of circulating every team over half of the cross-sections, was implemented in order to quantify the impact of site selection on the discharge measurement uncertainty.

Beyond the description of the experiments, uncertainty estimates are presented. The overall expanded uncertainty is estimated to be around  $\pm 6\%$  at 95% level of confidence for a measurement performed with 6 transects in the given measurement conditions of the experiments. However, the

uncertainty of the discharge measurements varies among the cross-sections. These variations are well correlated to the expert judgment on the cross-section quality made by each team. First results seems to highlight a relation between uncertainty computed for each cross-section and criteria such as the shallowness of the flow, the unmeasured discharge ratio.

Further investigations are necessary to identify the criteria related to error sources that are possibly meaningful for categorizing measurement conditions and site selection. Moreover, comparison between experimental uncertainty and analytical methods (such as computations recently proposed by QRev, Quant, Oursin or QMSys software) is planned to be done.



## Notation

*The following symbols are used in this report:*

- $A_r$  = the relative uncertainty half-interval of  $s_r$  estimate with a probability level of 95%;  
 $A_R$  = the relative uncertainty half-interval of  $s_R$  estimate with a probability level of 95%;  
 $B_i$  = the systematic (bias) error related to the  $i^{\text{th}}$  laboratory;  
 $c_i$  = the sensitivity coefficients related to the effects not covered in the experiments;  
 $k$  = the coverage factor used to expand the uncertainty to a given probability level;  
 $n$  = the average number of repeated measurements for each laboratory;  
 $n_i$  = the number of repeated measurements for the  $i^{\text{th}}$  laboratory;  
 $\bar{n}$  = the average number of repeated measurements per laboratory computed using Eq. G.5;  
 $N$  = the number of successive ADCP transects averaged to compute a discharge result;  
 $p$  = the number of participants involved in the interlaboratory experiment;  
 $P$  = the number of successive ADCP instruments averaged to compute a discharge result;  
 $Q$  = the discharge;  
 $Q_{i,k}$  = the  $k^{\text{th}}$  instantaneous discharge measurement of the  $i^{\text{th}}$  laboratory;  
 $\bar{Q}_i$  = the average of the repeated discharge measurements of the  $i^{\text{th}}$  laboratory;  
 $Q_{\text{mean}}$  = the average of all discharge values of the experiment;  
 $Q_{\text{ref}}$  = the reference discharge value;  
 $Q_{\text{true}}$  = the true discharge value (unknown);  
 $s_L$  = the estimator of the interlaboratory standard deviation;  
 $s_r$  = the estimator of the repeatability (intra-laboratory) standard deviation;  
 $s_R$  = the estimator of the reproducibility standard deviation;  
 $u(X)$  = the relative standard uncertainty associated with the quantity  $X$ ;  
 $U(X)$  = the expanded relative uncertainty associated with the quantity  $X$ , with a probability level of 95%;  
 $x_i$  = the input quantities related to the effects not covered in the experiments;  
 $y$  = the measurement result;  
 $\gamma$  = the reproducibility to repeatability ratio ( $\gamma = s_R/s_r$ );



$\delta$  = the bias associated with the measurement technique;

$\hat{\delta}$  = the estimator of the bias of the measurement technique;

$\varepsilon_{i,k}$  = the random error related to the  $k^{\text{th}}$  discharge measurement of the  $i^{\text{th}}$  laboratory;

$\sigma_L$  = the true interlaboratory standard deviation;

$\sigma_r$  = the true repeatability (intra-laboratory) standard deviation;

$\sigma_R$  = the true reproducibility standard deviation.



## 1. Introduction and objectives

Inter-laboratory experiments of discharge measurements are an useful tool to investigate the performance of a measurement technique and so a valuable tool for empirically estimating the uncertainty of stream gauging techniques in given measurement conditions. It consists of measuring the same variable (or discharge) with several participants, or laboratories, using the same measurement procedure. This chapter presents a summary of inter-laboratory experiments conducted in France since 2009 using ADCPs and current-meters. This chapter also presents the aims of "Chauvan 2016" experiments.

### 1.1 Review of inter-laboratory experiments

Since 2007, field inter-laboratory experiments have been conducted in the world of hydrometry, for instance in Germany, Canada, USA, England (Everard, 2007, 2009) or in Croatia (Terek et Nimac, 2008) and in France since 2009 under the leadership of *Groupe Doppler Hydrométrie*<sup>1</sup> (Le Coz *et al.*, 2009; Pobanz *et al.*, 2011; Hauet *et al.*, 2012; Pobanz *et al.*, 2015) and within government agencies. These field experiments were not only conducted using ADCPs but also using current-meters on wading rods in 2011 (Dramais *et al.*, 2011) and 2013 (Despax *et al.*, 2014, 2016).

In France, a particular aim is to empirically estimate the uncertainty of stream gauging techniques based on ISO standards (Le Coz *et al.*, 2016). Table 1.1 summarizes field experiments performed in France and associated uncertainty estimates.

ADCP uncertainty estimates range from 4 to 12 %. The maximum value comes from "Génissiat 2010" downstream of the dam with adverse measurement conditions (Pobanz *et al.*, 2015; Le Coz *et al.*, 2016) whereas, during the same experiments, the uncertainty estimate was lower at a more favorable site (Pyrimont). It highlights the importance of site selection and the need to estimate the uncertainty due to site effects and site selection.

---

<sup>1</sup>French-speaking community of hydrometry technologists.

Table 1.1: Review of inter-laboratory experiments performed in France. Uncertainties are expressed at a level of confidence of 95% and are based on 6 successive transect (4 for Génissiat 2010). Adapted from Dramais et al. (2013).

Experiment	Device	Discharge m <sup>3</sup> /s	Number of teams	Uncertainty (at 95%) %	Source
Vézère, 2009	ADCP (Tethered boats - bank-operated cableway)	30	37	4-9	(Le Coz <i>et al.</i> , 2009)
Génissiat, 2010 - Downstream of the dam - Pylimont site	ADCP (Mounted on boats)	110-430	26 12 14	4-12 8-12 4-6	(Pobanz <i>et al.</i> , 2011)
Gentille, 2011	ADCP (Tethered boats - bank-operated cableway)	10-20	34	6-7.5	(Hauet <i>et al.</i> , 2012)
Ouvèze, 2011 Toulourenc, 2011	Current-meter (wading rods)	1 0.4	11 11	15 16	(Dramais <i>et al.</i> , 2011)
Chooz, 2012	ADCP (Tethered boats - bank-operated cableway)	35	4	6	(Atmane, 2012)
Vaucluse, 2012	ADCP (Tethered boats - bank-operated cableway)	6	5	8-10	(Atmane, 2012)
Génissiat, 2012 - Downstream of the dam - Bognes site - Pylimont site	ADCP (Mounted on boats)	230-550	32 12 11 9	4-12 12 4.4 4.3	(Pobanz <i>et al.</i> , 2015)
Cernon, 2013 Durzon, 2013	Current-meter (wading rods)	0.8 1	12 13-11	11 10	(Despax <i>et al.</i> , 2014)

## 1.2 Objectives

The objectives of this study include:

- Comparing discharge measurements for all participants, and for each ADCP model,
- Comparing discharge estimates according to the cross-section,
- Sharing techniques and experiences,
- Estimating the uncertainty by applying field inter-laboratory experiments method,
- Evaluating the site selection impact on discharge measurement,
- Evaluating the impact of extrapolation coefficients,
- Comparing empirical uncertainty estimates with propagation methods.

To investigate the site selection effect and in contrast with earlier experiments, less favorable sites were selected (shallow water sites, obstacles).

To ensure a seamless data processing, data will be post-processed using QRev software (Mueller, 2016) including extrapol (Mueller, 2013).

Previous experiments have shown the impact of simultaneously using several ADCPs to decrease the uncertainty. One of the aims of this study is to evaluate the best strategy to reduce the uncertainty (using multiple cross-sections, using multiple ADCPs).



## 2. The experimental design

This chapter describes participants and ADCP gathered during the experiments and some logistical aspects.

### 2.1 Participants

50 teams including 7 foreign teams, deployed 50 ADCPs during these experiments. These teams include government agencies, private companies, research institutes and also some manufacturers. Some operators were professional field hydrologists with daily experience of ADCP measurements, whereas others worked with academic groups or consultant companies and use ADCPs more episodically. In the following report, each team is named using a four-letter code as follows:

- Compagnie d'Aménagement des Coteaux de Gascogne [CACG],
- Confederación Hidrográfica del Ebro [CHEB],
- Český hydrometeorologický ústav [CHMI],
- Compagnie Nationale du Rhône [CNR1 & CNR2],
- DREAL Grand-Est Strasbourg [ACAL],
- DREAL Angers [ANGE]
- DREAL Aquitaine [AQU1 & AQU2],
- DREAL Bretagne [BRE1 & BRE2],
- DREAL Centre Val de Loire [CVL1 & CVL2],
- DREAL Clermont-Ferrand [CLE1 & CLE2],
- DREAL Nantes [NAN1 & NAN2]
- DREAL Provence Alpes Côtes d'Azur [PAC1],
- DREAL Poitou-Charantes [VCA1, VCA2 & VCA3],
- DREAL Auvergne Rhône Alpes [ARA1 & ARA2]
- DRIEE Ile-de-France [IDF1 & IDF2],
- EDF-DTG (Grenoble, Toulouse and Brive) [CHA1, CHA2, CHP1, CHMC, FIXE],
- EDF R& D [RED1 & RED 2],
- Environment Agency UK [ENUK],

- EPTB Seine [EPTB],
- Hydro Sciences Montpellier [HSM1],
- Irstea (Aix, Bordeaux, Lyon) [IRSA, IRSB & IRSL],
- Korea Institute of Civil Engineering and Building Technology [KICT],
- M2E21 Dijon [M2E2]
- Norwegian Water Resources and Energy Directorate [NVE1],
- Q Measurement [QMEA],
- Société du Canal de Provence [SCP],
- Sveriges Meteorologiska och Hydrologiska Institut [SMHI],
- SonTek [STEK],
- SPC Grand Delta [SGD1 & SGD 2],
- Teledyne RDI [TRDI],
- Université de Tours [TOUR],
- USGS (USA) [USGS].

A group photo is presented in figure 2.1. Appendix B present of photograph of each team.



*Figure 2.1: Group photograph of all participants.*

The coordinating team was made up of 6 members (see figure B.2) to ensure the general organization, logistics, coordination of measurement tests, centralization of data, information, a link between power plant manager and the teams.

## 2.2 Equipment

### 2.2.1 ADCPs and tethered boats

5 kinds of ADCPs were used: M9 and S5 from SonTek manufacturer, StreamPro and RiverPro from Teledyne RDI and a Q-Liner constructed by OTT. Table 2.1 shows the number and few characteristics of each kind of ADCPs.

Table 2.1: Number of devices, technical characteristics and tethered boats. \* One M9 was replaced by a RiverPro during session # 2 (CHA1 team, due to a technical issue).

ADCP	Manufacturer	Number of AD-CPs	Frequency	Number of transducers	Echo-sounder	Boat
M9	SonTek	18*	3.0 MHz / 1 MHz	8	0.5 MHz	TorrentBoard, HydroBoard
S5	SonTek	1	3.0 MHz	4	1 MHz	HydroBoard
StreamPro	Teledyne RDI	26	2.4 MHz	4		Catamaran, Small Catamaran, RiverBoat
RiverPro	Teledyne RDI	4*	1.2 MHz	4	0.6 MHz	TorrentBoard
Q-Liner	OTT	1	2 MHz / 1 MHz	4		



Figure 2.2: ADCPs from below. (Sources: SonTek, Teledyne RDI, ASB Systems & Tecnologia y Ambiente).



Figure 2.3: ADCPs and associated tethered boats (from left to right: M9 mounted on HydroBoard, M9 on TorrentBoard, StreamPro on Small Catamaran, StreamPro on Catamaran and Q-Liner).

### 2.2.2 Software

Software requested versions: 2.10 (or newer) for WinRiver II and 3.6 (or newer) for RiverSurvey-online. Two teams provided discharge data computed using QRev (USGS and SMHI). Q-Liner measurements were computed using an in-house software (SCP).

A homogeneous discharge computation will be performed using QRev.

## 2.3 Logistics

### 2.3.1 Schedule

The inter-laboratory field experiments were conducted from 8th November to 10th November 2016. The day of 7th November was dedicated to the preparation of the site (installation of bank-operated cableways) and the preparation of the briefing. The schedule was as follows:

Tuesday 8 Nov:

- 9:00: Welcoming participants.
- 9:30-10:30: Housekeeping and safety instructions. Safety briefing with the EDF dam managers.
- 10:30-12:00: Installation of measurement equipment, test measurements to check that everything works well.
- 12:00-14:00: Lunch: "regional delicacy intercomparison" with products shared by participants, on site (see figure A.3).
- **14:00-17:00: 1st session of intercomparison measurements (session # 1).**
- 17:00-17:30: Wrap-up. Caretaking of the site by a private firm.
- Dinner.

Wednesday 9 Nov:

- 8:00: Welcoming participants.
- **8:30-12:00: 2nd session of intercomparison measurements (session # 2).**
- 12:00-14:00: Lunch provided by a caterer, on site.
- **14:00-17:00: 3rd session of intercomparison measurements (session # 3).**
- 17:00-17:30: Wrap-up.
- Dinner.

Thursday 10 Nov:

- 8:00: Welcoming participants.
- 8:00-9:30: Brief report of preliminary results of the experiments, on site.
- 9:30-12:00: Demonstration of equipment by manufacturers.
- 12:00-13:00: Lunch provided by a caterer, on site. End of the intercomparison event.
- 14:00-18:00: International hydrometry workshop (Saint-Marc dam, see program at section 2.3.2).

### 2.3.2 International hydrometry workshop

The program was as follows:

- Mikael Lennermark (SMHI, Sweden) – ADCP measurements: improving measurement results with a higher voltage on the StreamPro (18V) and also about the quite common flow disturbance in the top cell.
- Chanjoo Lee (KICT, Korea) – River Experiment Centre, the unique controllable testing facility for evaluation of ADCPs.
- Kevin Oberg and Frank Engel (USGS, USA) – QA/QC using QRev - SurfBoard.
- Kristoffer Florvaag-Dybvik and Trine Lise Sorensen (NVE, Norway) - Impact of Extrap application on NVE reported discharge and flow disturbance on a still lake.
- Nick Everard (Environment Agency, UK) – ADCP test events in the UK in 2016, and benefits of RC boats to ADCP flow measurements, with focus on 2013/14 floods.
- José Ramón Sánchez Puertas (CH Ebro, Spain) – Some experiences with LSPIV using flood movies.

- Jérôme Le Coz (Irstea, France) - Non contact velocimetry techniques for flood gaugings (LSPIV and SVR).
- Gilles Pierrefeu (CNR, France) - OURSIN : OURSIN : Uncertainty repartition tool for ADCP measurements - OUtil de Répartition deS INcertitudes de mesure de débit par ADCP mobile.

### 2.3.3 Safety

The tests were conducted downstream of the Chauvan dam. As the dam managers, EDF control the released flows and the risks due to water rise around the site. Every team must ensure their own safety while measuring discharge next to the water course: EDF takes no responsibility for that. To achieve the measurements, everyone are requested to wear life jackets and suitable shoes, since the ground is uneven and slippery when rainy. At least two operators are requested to conduct a measurement.

Four members of the coordinating team ensure smooth and safe operations from the bank. A communication is maintained between dam managers and each team. During nights, a security guard was assigned for caretaking.

No incidents or injuries were registered during the experiments.

**Note:** for safety and logistical reasons, the number of registered teams were limited to 50.

## 2.4 Site presentation

The inter-laboratory experiments were conducted on the Taurion River (right hand side tributary of the Vienne River), downstream of EDF-operated Chauvan Dam, at Saint-Priest-Taurion, Haute-Vienne, France (figure 2.4 and table 2.2).

*Table 2.2: Geographic site information.*

<b>District (Department)</b>	Haute-Vienne (71)
<b>Town (Locality)</b>	Saint-Priest-Taurion (Chauvan)
<b>Latitude</b>	45.9046 N
<b>Longitude</b>	1.4108 W
<b>Altitude</b>	246 m

A tent was mounted to install the organization team headquarters, to gather participants and for lunches.

### 2.4.1 Cross-sections

26 cross-sections with various shapes and flow conditions and more or less favorable conditions, were distributed over 500 m along the Taurion River and equipped with ropes and pulleys. Cross-sections were about 35 m wide and 1 m deep. Each cross-section was named with a letter (from A to X). Figure 2.5 shows the 24 cross-sections where participants were circulated. Two teams deployed their ADCP continuously during each session using a Q-Liner and a StreamPro respectively at two "fixed" cross-sections named SCP and FIXE close to EDF-DTG hydrometric station. Appendix C.1 shows photographs (looking downstream and upstream) of each cross-section.





Figure 2.4: View of site, Chauvan Dam, the tent, the car park and Taurion River (Source: N. Everard, UK Environment Agency).



Figure 2.5: Location of each cross-section (OpenStreetMap). The blue triangle shows the EDF-DTG hydrometric station.

## 2.5 Evaluation of the cross-section quality

During measurements, each team made a judgment about the quality of each cross-section they measured: poor, fair or good. Figure 2.6 shows the scores of all cross-sections.

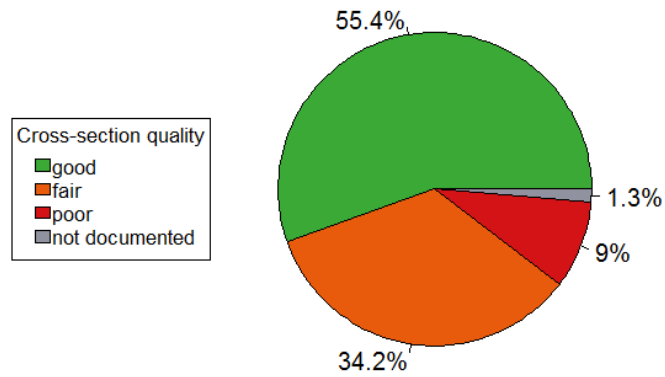


Figure 2.6: Chart showing quality evaluation of all cross-sections.

More than half of the cross-sections were considered as good cross-sections and only 9 % as poor.

### 2.5.1 By teams

For information, figure 2.7 shows quality evaluations assigned by each team. It highlights the subjectivity of this analysis since each team has a different appreciation of standard of quality.

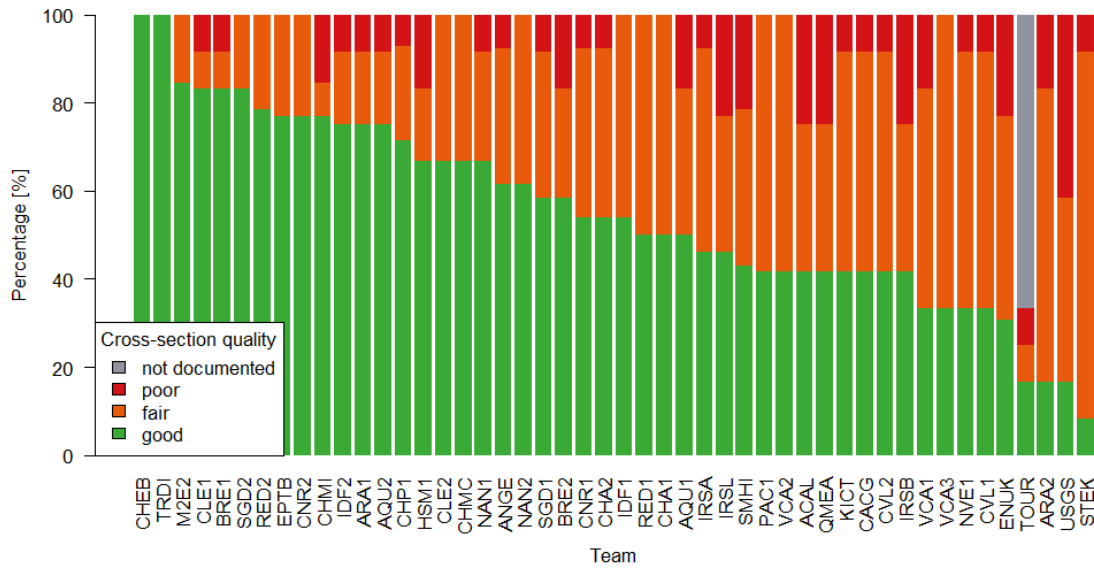


Figure 2.7: Distribution of votes from each team.

2.5.2 By cross-sections

Figure 2.8 shows the quality evaluation for each cross-section.

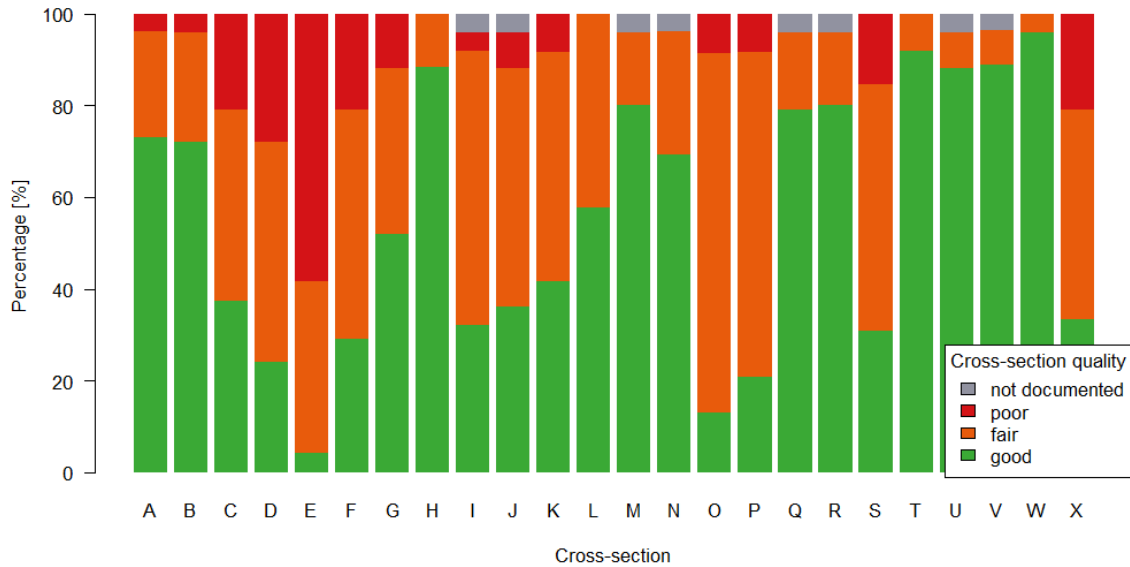


Figure 2.8: Distribution of votes on the quality of each cross-section (from upstream to downstream).

Figure 2.9 shows the classification of the cross-sections ranked by the quality evaluation: good (figure 2.9a) or poor (figure 2.9b).

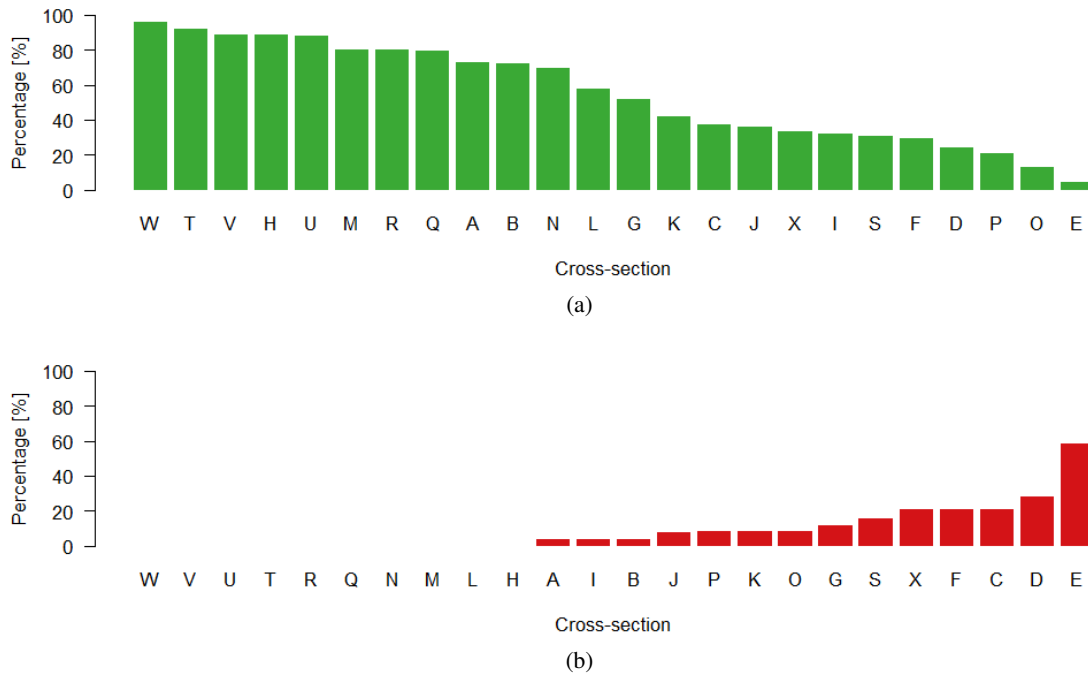


Figure 2.9: Proportion of votes for each cross-section ranked by quality: (a) good or (b) poor.

It seems clear that cross-section E was considered as the worst cross-section. This is explained by the presence of a tree upstream of the cross-section (figure 2.10) that created eddies. This cross-section is also the shallowest.



Figure 2.10: Panoramic photo of cross-section E (Source: N. Everard, UK Environment Agency).

## 2.6 Measurements

### 2.6.1 Hydraulic conditions

A constant discharge (around  $14 \text{ m}^3/\text{s}$ ) was released by the dam during the 3 measurement sessions. During session 1 and 2, the discharge was released by turbo-generators number 1 and 2 respectively. During session 3, the discharge was released directly by a dam spillway, as illustrated on figure 2.11, resulting in slightly different discharges. Results will be corrected to allow comparison and uncertainty computation (see section 3.6).



Figure 2.11: Discharge released by dam spillway (session # 3) (Source: A. Despax).

A minor tributary was observed between sections M and N. Its discharge was estimated at between  $0.01$  and  $0.02 \text{ m}^3/\text{s}$  according to current-meter measurements. During session 2, a screening operation (to flush organic matter) caused the spill of around  $0.40 \text{ m}^3/\text{s}$  during less than 5 minutes.

### 2.6.2 Water-level monitoring and additional measurements

Water level control was monitored at three locations: at cross-section X and P by differential piezometer gauges (Paratronic) and at the gauging station by a radar gauge (VEGA). Stage was also periodically read at staff gauge. The hydrometric station is located upstream of a weir. By applying a stage-discharge relation (or rating-curve), water level recorded was into discharge.



Figure 2.12: EDF-DTG hydrometric station with VEGA radar gauge (Source: A. Despax).

Dye dilution gaugings (using fluorescein tracer, see picture 2.13) were performed during tests.

In addition, two teams (SCP and FIXE) deployed their ADCPs at two cross-sections using a Q-Liner (OTT), section-by-section method, and a StreamPro respectively (Teledyne RDI).



Figure 2.13: Dye dilution gauging downstream of the dam (Source: A. Despax).

### 2.6.3 Measurement sessions - experimental plan

The experimental design consisted in circulating every team over half of the cross-sections during three sessions of measurements. For each session, a road map was designed for each team with 4 compulsory cross-sections to be measured and 4 additional cross-sections if time allowed. The road map was given at the beginning of each measurement session in tabular form (paper and numeric versions, see appendix D.2). All information, such as time at the beginning and end of the measurement, number of valid transects, mean discharge, standard deviation of transects, evaluation of cross-section quality (poor / fair / good) and measured discharge ratio (measured discharge over total discharge), was included in this form.

At the end of each session, the data (paper and numeric format) were collected to present live preliminary results. Both raw data and summary of each measurement were collected. Incident sheets were also completed by the coordinating team (see appendix D.1).

ADCP models were spread evenly among the 24 cross-sections so that each cross-section was measured by an equivalent number of ADCPs from the two manufacturers.

In practice, each team measured the discharge at 12 cross-sections at least during each session. The distribution of measurements depending on the team, the cross-section and ADCP device is presented in figure 2.14. The average number of measurements by a team is 24, as each team measured the discharge at half of all cross-sections, as planned.

Before each session, the team checked the computer time and the charge level of batteries. Compass calibration and system test were also requested. The number of valid transects were initially set at 8 (4 reciprocal pairs of transects). Given the measurement time related to this number of transects, it was reduced to 6 (3 pairs of measurements with reciprocal courses). In practice, two teams were present at the same cross-section, one performing a measurement and the other waiting.

Configuration of the ADCP, edge distance estimation and edge extrapolation choices were free. Although some ADCPs were coupled with GPS, bottom tracking reference was imposed to compute the discharge.

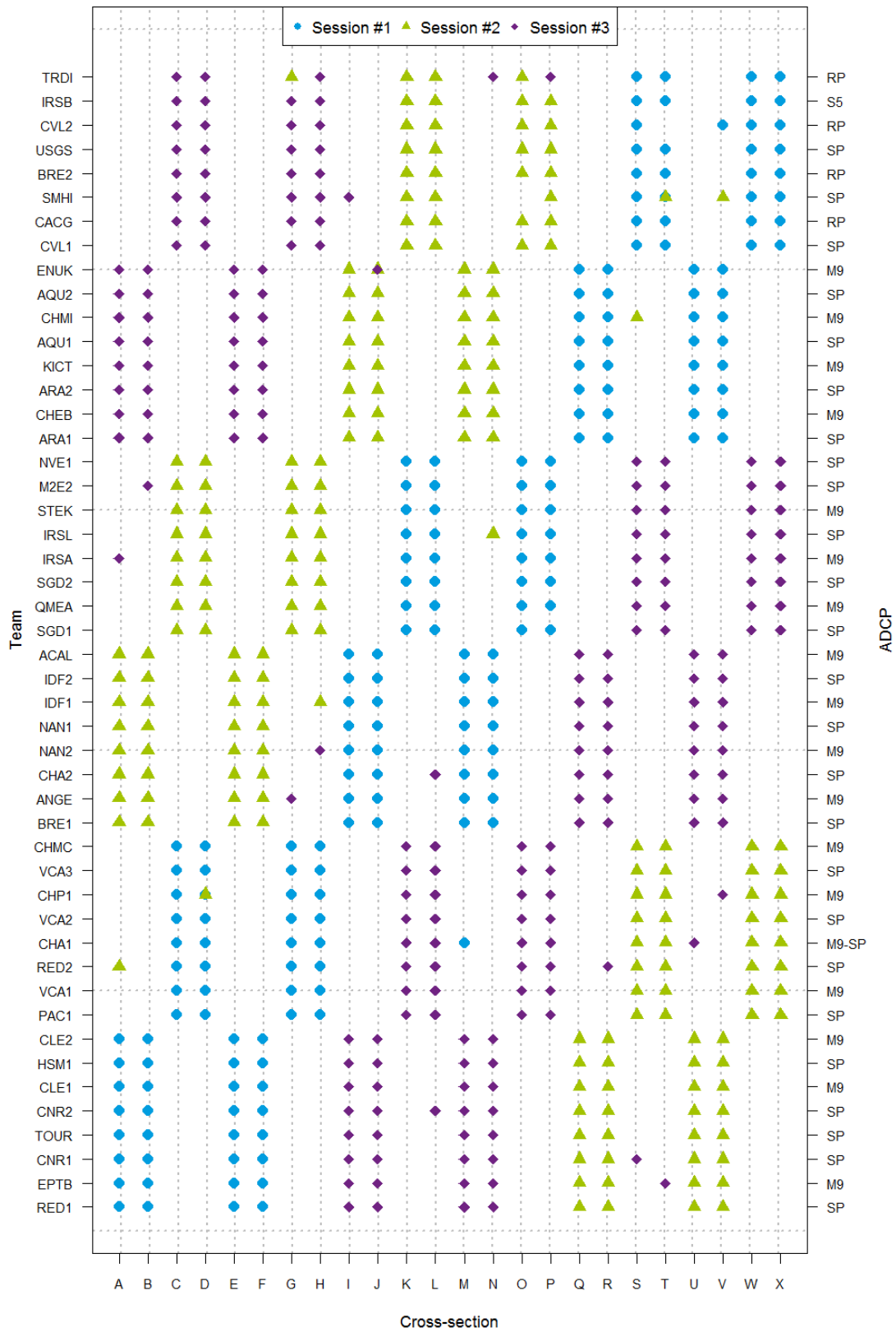


Figure 2.14: Distribution of all the measurements depending on the team, the cross-section and ADCP model (on the right side).

## 3. Results

### 3.1 Stage time series

Stage was monitored at three locations along the reach (at cross-sections P, X and at the hydrometric station, upstream of the weir). At these 3 sites, stage time series are presented in figure 3.1 and 3.2.

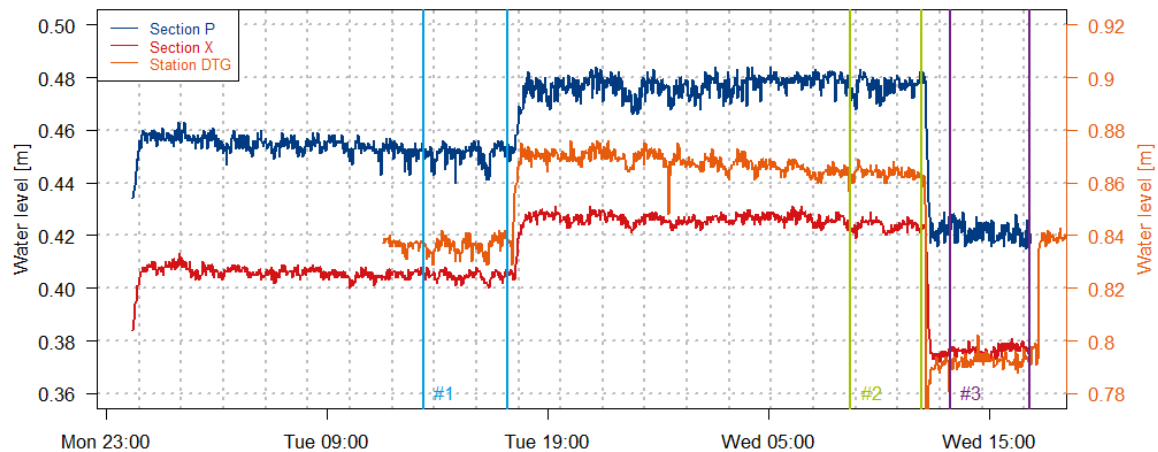


Figure 3.1: Stage time series observed at EDF-DTG hydrometric station and cross-sections P and X.

The analysis of the stage time series highlights a satisfactory stability of water stage during all the measurement sessions. Water level variations were less than 1 cm at cross-section X and at EDF-DTG hydrometric station. The cross-section P was more sensitive to discharge variations. However water level variations are of the same order (maximum around 1 cm). This analysis reflects a steady state flow during each of the 3 sessions. It also shows that discharge stability was reached at all cross-sections from upstream to downstream.



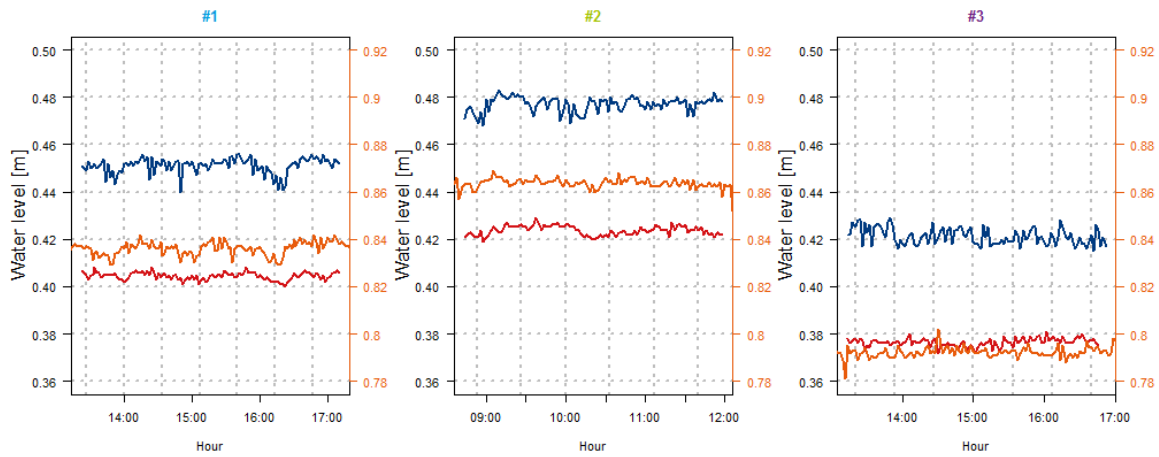


Figure 3.2: Stage time series observed at EDF-DTG hydrometric station and cross-sections P and X for each measurement session.

Table 3.1 summarizes the statistics computed on water level recorded at EDF-DTG hydrometric station.

Table 3.1: Statistics in terms of minimum, first quartile, median, mean, third quartile, maximum and standard-deviation of water levels measured at EDF-DTG hydrometric station, in *m*.

Session	Min.	1st Quartile	Median	Mean	3rd Quartile	Max.	Standard-deviation
# 1	0.829	0.834	0.836	0.836	0.838	0.842	0.003
# 2	0.767	0.862	0.863	0.860	0.865	0.869	0.017
# 3	0.788	0.791	0.792	0.793	0.793	0.802	0.002

### 3.2 Flow steadiness

The transformation of a stage time series into chronicle of flow time series is based on a stage-discharge relation (rating curve) at the hydrometric station. For the observed stages, the stage discharge relationship is controlled by a weir (figure 2.12). Figure 3.3 shows three different rating-curves obtained by a classical method (named EDF-DTG rating-curve), GesDyn method (Morlot, 2014; Morlot *et al.*, 2014) and BaRatin method (Le Coz *et al.*, 2014) with associated uncertainty (at 95% level of confidence).

A list of gaugings used to plot these rating-curves is presented in table E.1. Almost all the gaugings were performed using StreamPro ADCPs deployed at cross-section labeled FIXE upstream of the weir (see 2.5). Thus, the comparison between ADCP measurements during Chauvan experiments, especially StreamPro ADCP measurements performed at cross-section FIXE, and flow time series should be interpreted carefully given the dependency of these discharge estimates.

Figure 3.4 shows discharge time series associated with different rating-curve models:

- Manually-built rating-curve currently used at EDF-DTG hydrometric station,
- Dynamic rating curve obtained based on GesDyn approach,
- Bayesian analysis of rating curves (BaRatin).

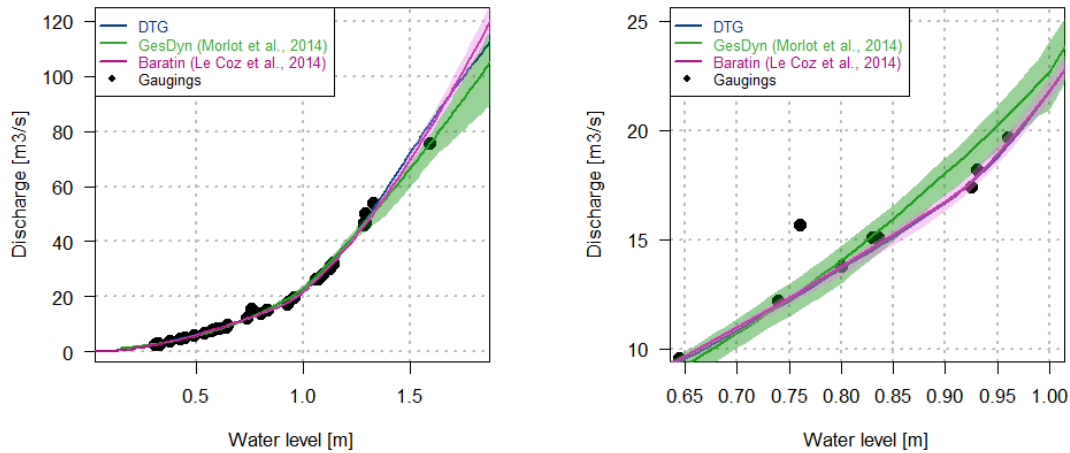


Figure 3.3: Gaugings and rating-curves with associated uncertainty (at 95% confidence level). On right side: logarithmic scale. Note: further investigation is needed to analyze differences between all curves.

Discharge estimates based on rating-curves for averaged observed water level are presented in table 3.2.

Table 3.2: Discharge and associated uncertainty (at 95%) computed using averaged observed water level for the 3 sessions (\* Confidence intervals are given in brackets).

Session	Averaged level m	DTG m <sup>3</sup> /s	GesDyn (CI*) m <sup>3</sup> /s	BaRatin (CI*) m <sup>3</sup> /s
# 1	0.84	14.81	15.57 (14.53 - 16.22)	14.93 (14.04 - 15.77)
# 2	0.86	15.40	16.36 (15.35 - 17.02)	15.53 (14.60 - 16.40)
# 3	0.79	13.43	13.69 (12.68 - 14.36)	13.47 (12.70 - 14.24)

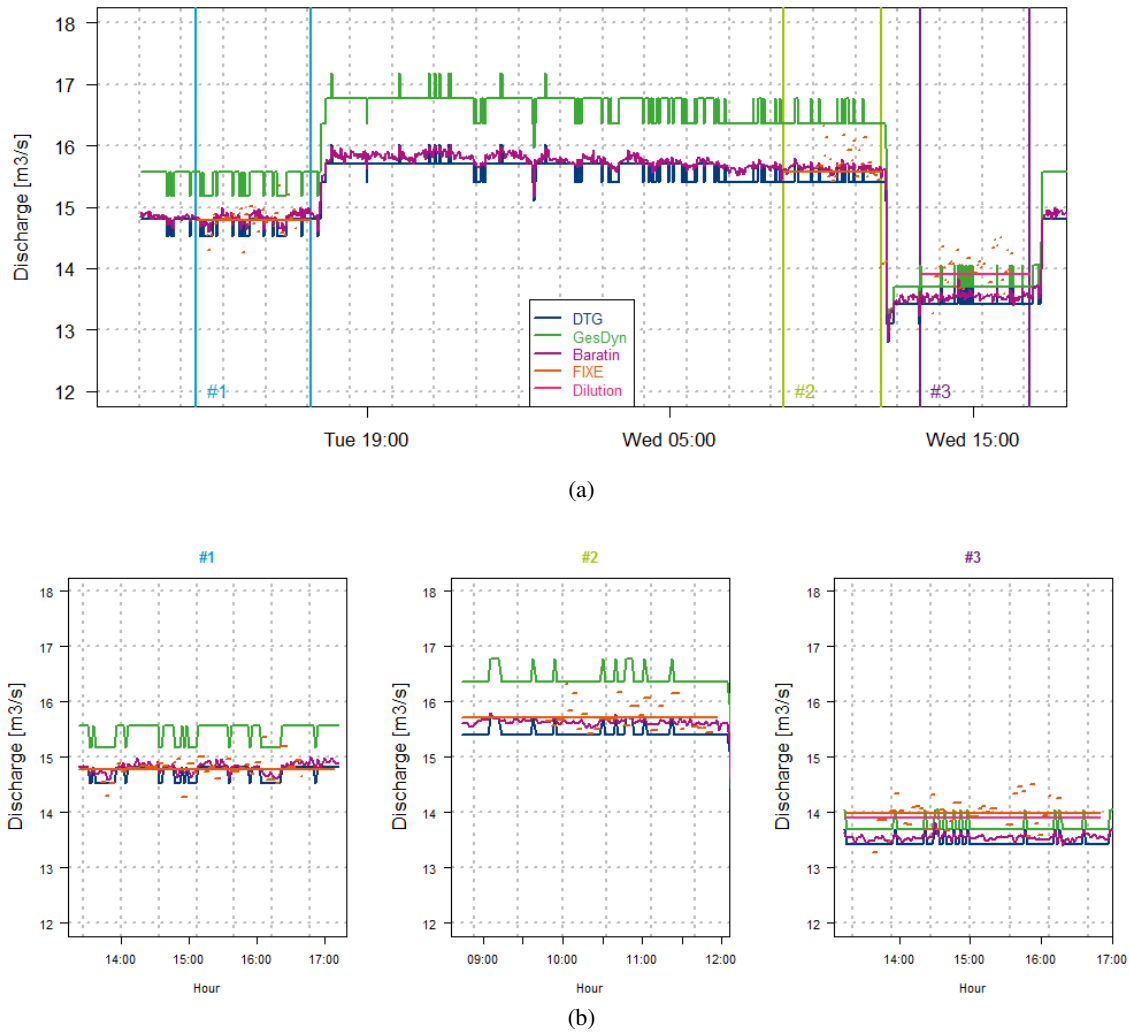


Figure 3.4: Flow time series associated with EDF-DTG rating-curve, GesDyn method and BaRatin method (a) during the whole event and (b) by session. Discharge measurements performed by team FIXE (see section 3.3.3) are displayed in orange (segments represent each measurement while solid horizontal lines show the mean discharge per session).

$S_Q$ , expressed in  $\text{m}^3/\text{s}$ , is defined as the sensitivity of the hydrometric station. It represents the variation of discharge induced by a variation of 1 cm in water level. Computed sensitivities are presented in table 3.3 for each rating-curve and each session. For water height of 0.85 m, the sensitivity is about  $0.30 \text{ m}^3/\text{s}/\text{cm}$ .

Table 3.3: Rating-curve discharge sensitivity for each session, expressed in  $\text{m}^3/\text{s}/\text{cm}$ .

Session	EDF-DTG $\text{m}^3/\text{s}$	GesDyn $\text{m}^3/\text{s}$	BaRatin $\text{m}^3/\text{s}$
# 1	0.29	0.39	0.29
# 2	0.30	0.40	0.30
# 3	0.30	0.36	0.29

### 3.3 Independent discharge measurements

#### 3.3.1 Dye dilution gaugings

Dye dilution gaugings (using fluorescein tracer, see picture 2.13) were tried. However, due to insufficient tracer mixing, discharge estimates from measurements performed on sessions 1 and 2 are not valid.

During session 3, a dye dilution gauging yielded to a  $13.90 \text{ m}^3/\text{s}$  discharge estimate. The tracer mass was 18 g for a distance between injection point and probes of 800 m approximately. Appendix F presents the details of this gauging.

#### 3.3.2 Section by section ADCP measurements

Team SCP measured the discharge continuously at the same cross-section labeled SCP in figures 2.5 and C.1, upstream of the weir, using a section-by-section ADCP Q-Liner (OTT manufacturer). Discharge measurements are summarized and compared with other discharge estimates in table 3.4.

#### 3.3.3 Continuous ADCP measurements

Similarly, the team named FIXE performed 35, 32 and 42 discharge measurements during sessions 1, 2 and 3 respectively. Their cross-section is also located upstream of the weir (see figures 2.5 and C.1). This cross-section was a good site to measure the discharge since the measured discharge ratio was about 71%. A transect is shown on figure 3.5, as an example. Due to low velocities near the edges, right and left extrapolated discharges are negligible ( $\ll 1\%$  of total discharge).

The mean discharge computed for each session is presented in table 3.4 and shown on figure 3.4. Further investigations using QRev software will be performed regarding the estimation of extrapolation coefficients (bottom and top layer). Preliminary tests show a reduction of discharge estimate ( $-2\%$ ) by applying QRev automatic fit extrapolation.

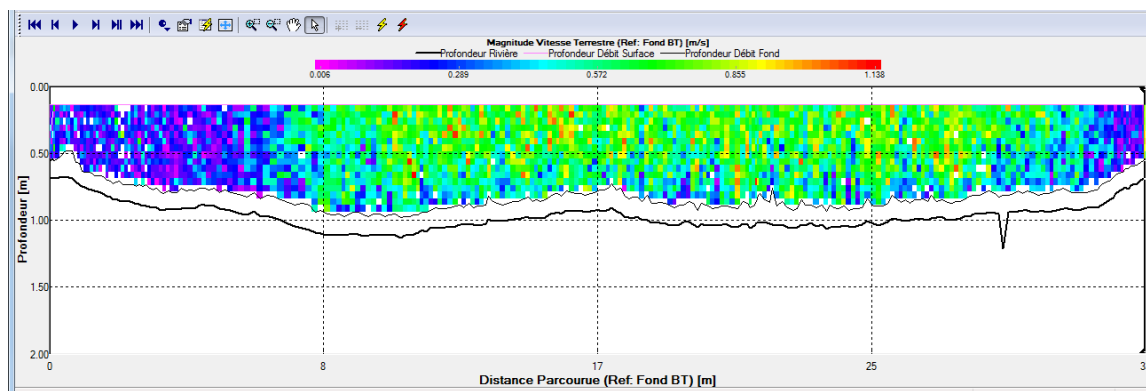


Figure 3.5: Transect measured by team FIXE during session # 1 (Extract from WinRiver software).

### 3.4 Summary of discharge estimates

Table 3.4 summarizes discharge values during each session estimated from rating-curves, dye dilution or continuous ADCP gaugings (SCP and FIXE teams).

Table 3.4: Summary of discharge results, expressed in  $m^3/s$ . \* number of measurements performed are given in brackets.

Session	DTG $m^3/s$	GesDyn $m^3/s$	BaRatin $m^3/s$	Dye dilution $m^3/s$	SCP* $m^3/s$	FIXE* $m^3/s$
# 1	14.81	15.57	14.93		15.91 (4)	14.78 (35)
# 2	15.40	16.36	15.53		15.27 (3)	15.72 (32)
# 3	13.43	13.69	13.47	13.90	14.45 (4)	13.99 (42)

### 3.5 ADCP measurement results

#### 3.5.1 Results for each session

Table 3.5 summarizes statistics computed on ADCP discharge measurements performed by the 48 teams of operators. For each session, the standard-deviation is about  $0.4 m^3/s$  which corresponds to an increase of 1 cm at the hydrometric session. This dispersion may be explained by the water level unsteadiness observed during the sessions (see section 3.1).

Table 3.5: Number of ADCP discharge measurements, number of transects, mean, standard-deviation, minimum and maximum discharge values during each session.

Session	ADCP measurements	Valid transects	Mean $m^3/s$	Standard-deviation $m^3/s$	Min $m^3/s$	Max $m^3/s$
# 1	193	1345	14.85	0.44	13.52	16.32
# 2	198	1149	15.63	0.49	13.85	17.00
# 3	206	1247	13.81	0.42	12.30	15.02

Table 3.6 presents a comparison between the average of all ADCP measurements and independent discharges estimates. Differences between ADCP measurements (from 48 teams) with EDF-DTG rating-curve and with BaRatin rating-curve are similar but lower than differences observed between ADCP measurements with SCP measurements and with discharge estimated using GesDyn rating-curve. Differences with SCP measurement might be explained by a not suitable velocity extrapolation coefficient. Lastly, differences between ADCP measurements and the continuous StreamPro measurements (FIXE team) are very small. This comparison does not allow us to estimate a potential bias since both measurements are based on the same ADCP technique. On the other hand, the small difference observed with dye dilution gauging suggest the bias is small.

Table 3.6: Differences between independent discharge estimates and averaged ADCP measurements by session, expressed in %.

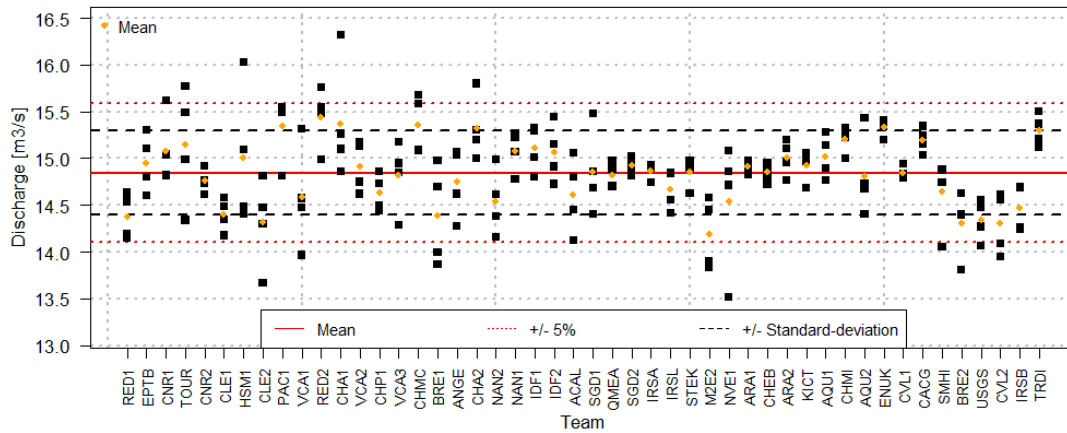
Session	Mean discharge $m^3/s$	DTG %	GesDyn %	BaRatin %	Dilution %	SCP %	FIXE %
# 1	14.85	-0.3	-4.6	+0.5		+7.1	-0.4
# 2	15.63	-1.5	-4.5	-0.6		-2.3	+0.6
# 3	13.81	-2.8	+0.8	-2.4	+0.6	+4.6	+1.2

### 3.5.2 Results for each team

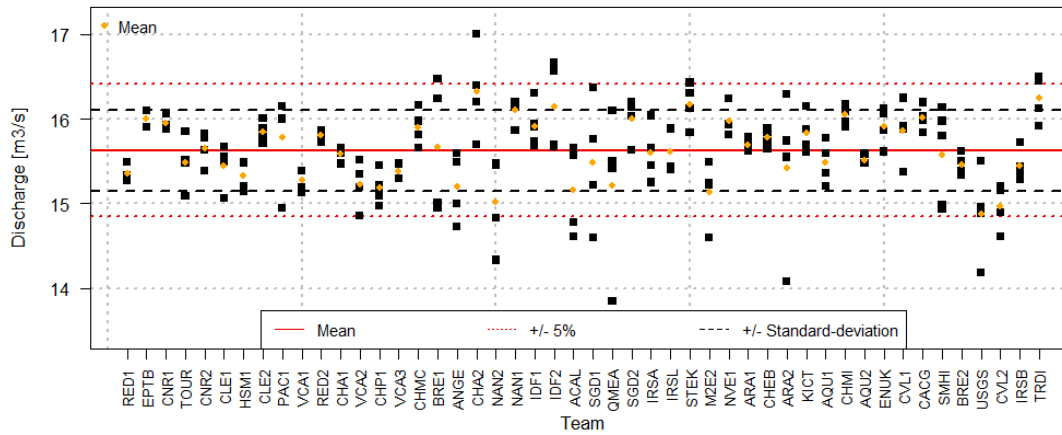
Discharges measured by each team are presented on figure 3.6. Most of these measurements are within  $\pm 5\%$  around mean discharge.

### 3.5.3 Results for each cross-section

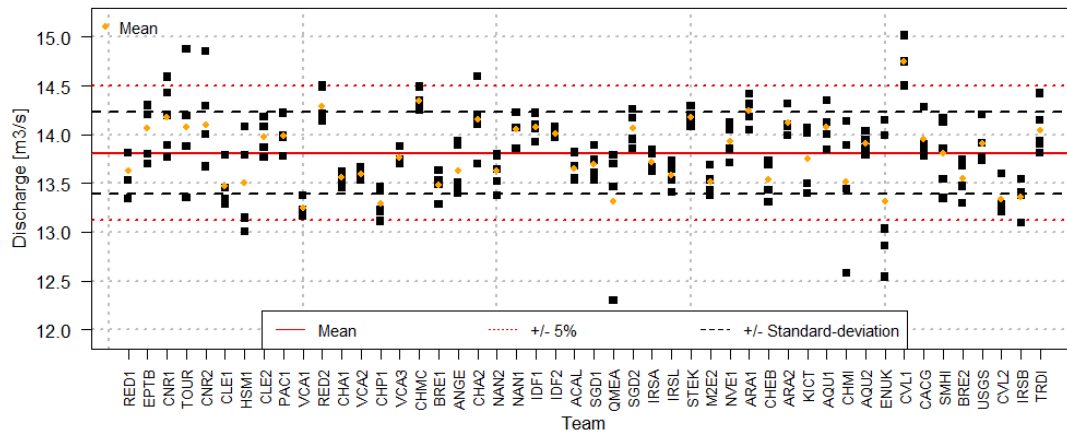
Discharge estimates depending on the cross-section are shown on figure 3.7 for each session. Discharges are less scattered for the most upstream and the most downstream cross-sections.



(a) Session # 1

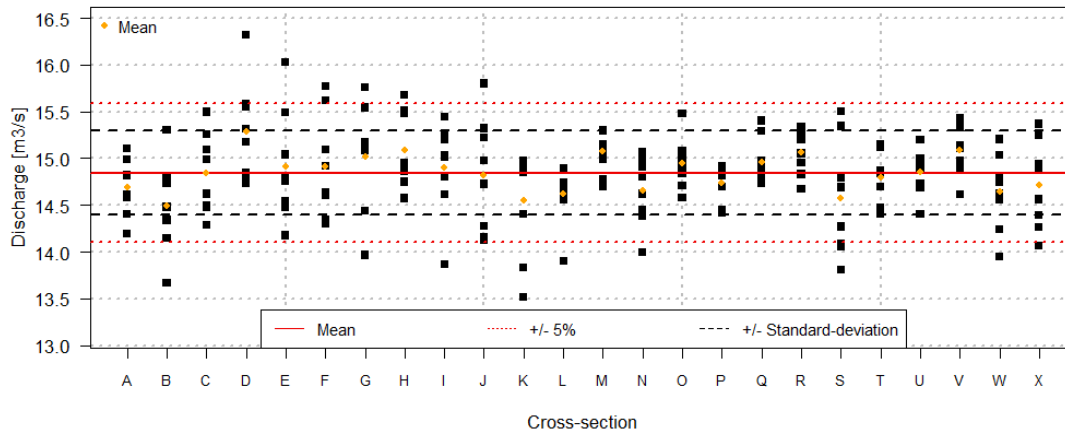


(b) Session # 2

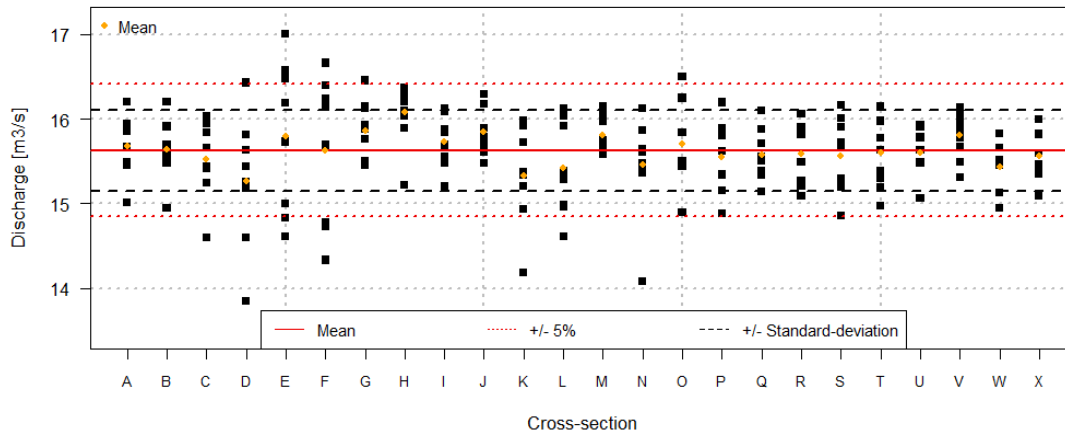


(c) Session # 3

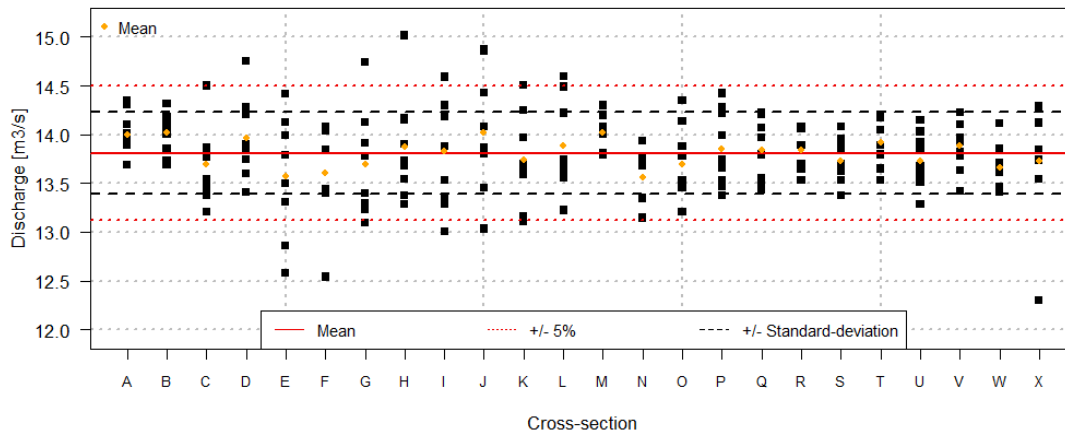
Figure 3.6: Discharge measurements of the 48 teams for sessions # 1 (a), 2 (b) and 3 (c).



(a) Session # 1



(b) Session # 2



(c) Session # 3

Figure 3.7: Discharge measurements of the 24 cross-sections for sessions # 1 (a), 2 (b) and 3 (c).



### 3.6 Corrected discharge estimates

During the three sessions of measurement, mean discharges were slightly different (see table 3.5) due to different ways of releasing discharge (see section 2.6.1). However, the streamflow was steady during all the sessions. It allows us to correct discharge estimates to analyze them homogeneously regardless the session. For that purpose, corrected discharge  $\widehat{Q}_{i,j,k}$  is defined as:

$$\widehat{Q}_{i,j,k} = Q_{i,j,k} - \left( \overline{Q}_k^{(i,j)} - \overline{Q}^{\equiv(i,j,k)} \right) \quad (3.1)$$

where  $Q_{i,j,k}$  is the  $j$ -th discharge measurement performed by the  $i$ -th team number  $i$  during the  $k$ -th session,  $\overline{Q}_k^{(i,j)}$  is the mean of all discharge measurements performed during session  $k$  and  $\overline{Q}^{\equiv(i,j,k)}$  is the averaged value of all discharge measurement during all sessions ( $14.75 \text{ m}^3/\text{s}$ ).

Processing such corrected discharges altogether is possible since the streamflow steadiness was checked and differences in terms of mean discharges between each session are similar and small. The error sources and the error model are supposed to be the same.

#### 3.6.1 Corrected discharge values by team

Results in terms of corrected discharges depending on the team are shown on figure 3.8. A homogeneous discharge computation will be applied later on using QRev software. This post-processing will probably lead to modifications in terms of discharges computed.

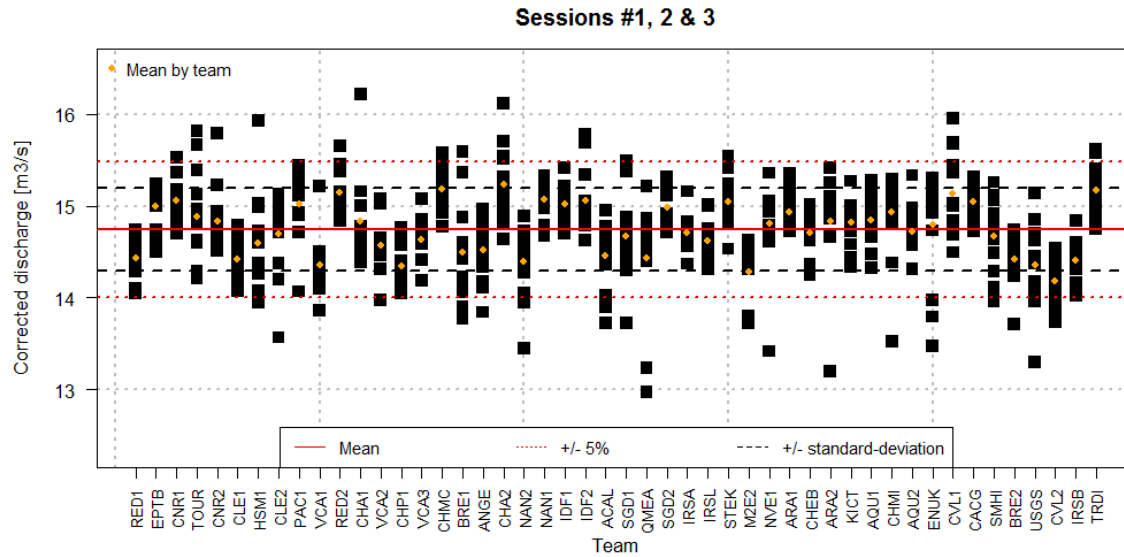


Figure 3.8: Corrected discharge values measured by the 48 teams (all sessions taken together).

#### 3.6.2 Corrected discharge values by cross-section

Results in terms of corrected discharges depending on the cross-section are shown on figure 3.9.

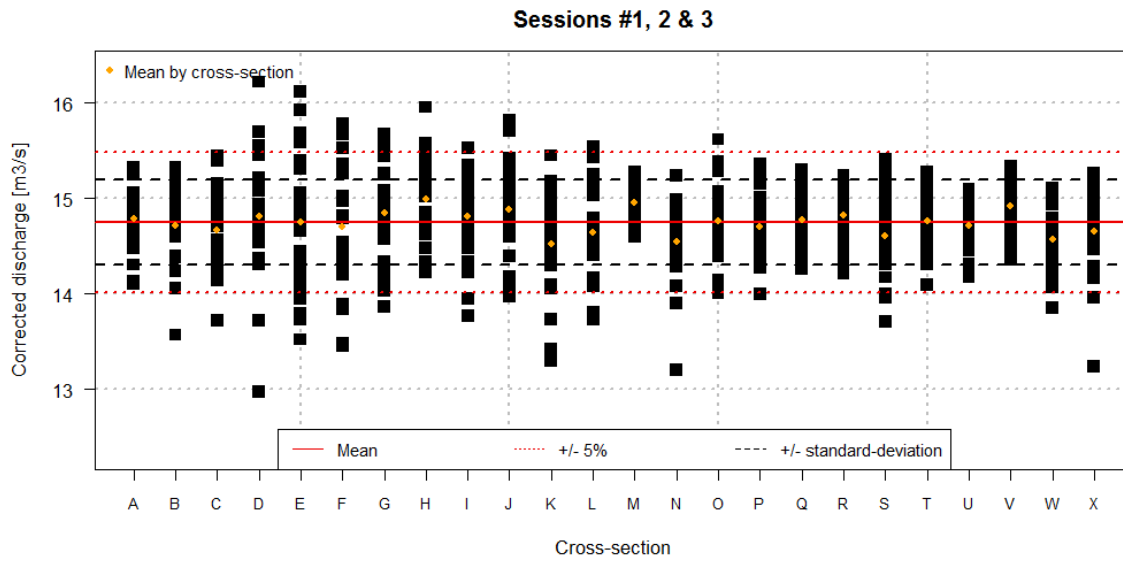


Figure 3.9: Corrected discharge values measured at the 24 cross-sections (all sessions taken together).

Cross-sections M and V present the smallest dispersion of discharge values. On the other hand, cross-sections E and D give a very large dispersion of discharge data. In terms of bias, the mean discharges computed from cross-sections B, E, T and O are the closest to the mean discharge computed using all the discharge values. Dispersion (standard-deviation) and deviation from the mean are presented in section 4.1. It should be reminded that QRev post-processing will slightly modify discharge values.

### 3.6.3 Measured discharge ratio by cross-section

Figure 3.10 shows the measured discharge ratio (measured discharge over total discharge) depending on the cross-section. The median measured discharge ratio is between 57 and 67 %. Cross-sections U, W, R and Q have the highest median measured discharge ratio values.

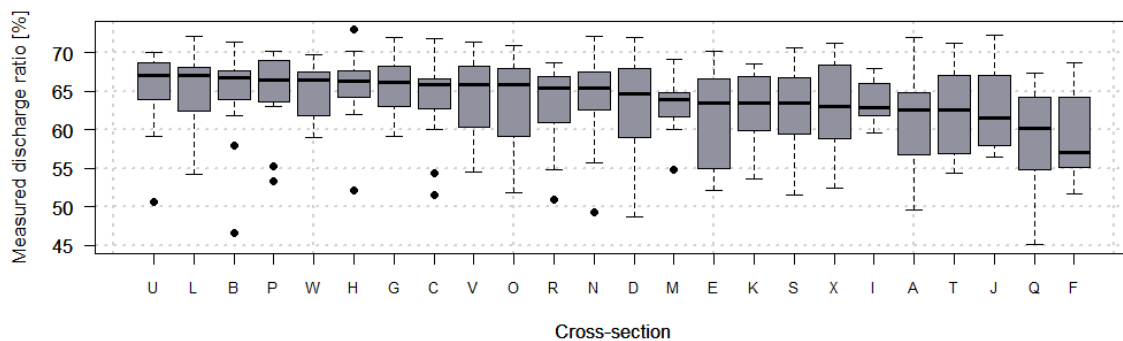


Figure 3.10: Boxplots showing measured discharge ratios of the 24 cross-sections (cross-sections are ranked based on median ratio values.)

There is a link between discharge dispersion and measured discharge ratio (figure 3.9). Cross-sections U and W which have the highest measured discharge ratios present a small dispersion of discharge values. These cross-sections were also qualified as good (figure 2.9a). On the other hand, cross-section E has a small measured discharge ratio and a high discharge dispersion. This cross-section is the poorest one according to operator evaluations (figure 2.9b). However, cross-section D, with a pretty high measured discharge ratio, has a high discharge dispersion. Further investigation, based on QRev post-processing, will be necessary to explain this conclusion. Default extrapolation coefficients set by operators are probably not suitable for this site. Supervised analysis of vertical velocity profiles will probably lead to new values of discharge.



## 4. Preliminary analysis

### 4.1 Statistical analysis

#### 4.1.1 Dispersion of results for each team

Let  $i = x + y$  with  $x$  (from  $x = 1$  to 24) the cross-section index and  $y$  the team index (operator and ADCP,  $y = 1$  to 48). The standard-deviation of discharges measured by a team  $y$ ,  $s_y$ , is computed as:

$$s_y^2 = \frac{1}{n_y - 1} \sum_{y=1}^{n_y} \left( \widehat{Q}_{x,y,j,k} - \overline{\overline{\overline{Q}}}_{x,j,k} \right)^2 \quad (4.1)$$

with  $n_y$  the number of measurements performed by a team  $y$  during the sessions and  $\widehat{Q}_{x,y,j,k}$  their corrected discharge measurement (see equation 3.1).  $\overline{\overline{\overline{Q}}}_{x,j,k}$  is the average of corrected discharges measured by team  $y$ .

Figure 4.1 shows the dispersion of corrected discharge values depending on the team. The dispersion is relatively small. The wider dispersion observed for some teams is possibly due to the fact that these teams measured discharge at worse cross-section compare to other teams. QRev post-processing will probably correct discharge values and affect these results.

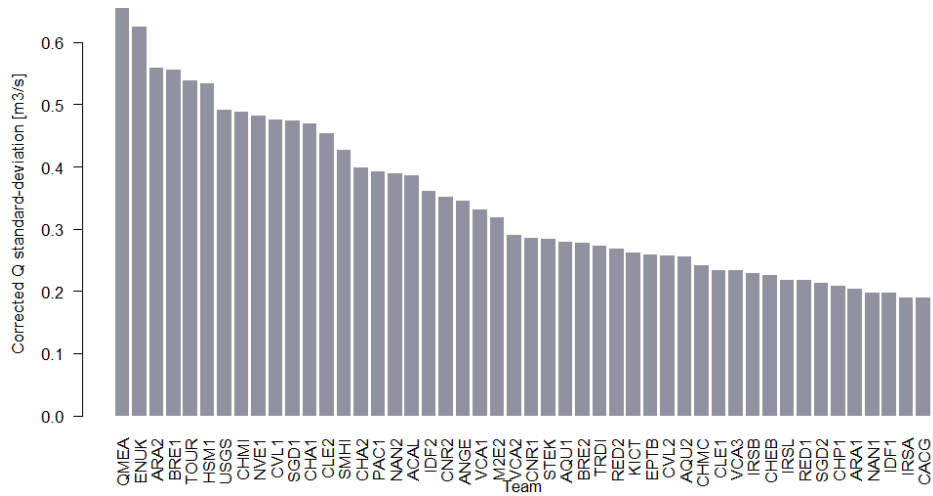


Figure 4.1: Standard-deviation of corrected discharge values depending on the team (ranked by descending order).

#### 4.1.2 Dispersion and deviation by cross-section

Let  $s_x$  and  $B_x$  computed as:

$$s_x^2 = \frac{1}{n_x - 1} \sum_{x=1}^{n_x} \left( \widehat{Q_{x,y,j,k}} - \overline{\overline{\overline{Q_{x,y,j,k}}}} \right)^2 \quad B_x = \overline{\overline{\overline{Q_x^{(y,j,k)}}}} - \overline{\overline{\overline{Q^{(x,y,j,k)}}}} \quad (4.2)$$

with  $n_x$  the number of measurements performed on section  $x$  (all sessions together) and  $\widehat{Q_{x,y,j,k}}$  the corrected discharge (estimated according to equation 3.1).  $\overline{\overline{\overline{Q_x^{(y,j,k)}}}}$  is the average of corrected discharges measured at cross-section  $x$  and  $\overline{\overline{\overline{Q^{(x,y,j,k)}}}}$  the average of all corrected discharges.

Figures 4.2 and 4.3 show average deviation from the mean ( $B_x$ ) and standard-deviation of corrected discharge ( $s_x$ ) depending on the cross-section (equations 4.2). Figure 4.2 seems to show that discharge estimates at cross-section H are biased (under-estimated) whereas mean discharge computed at cross-section B is very close to the average of all measurements. However, average deviations from the mean are lower than 2% and Qrev post-processing will possibly change this bias.

Figure 4.3 highlights cross-sections that give higher dispersion in terms of corrected discharge. Thus, discharges estimated at cross-sections E, D and F are very scattered compared to cross-section M (standard-deviation lower than 0.20 m<sup>3</sup>/s). Once again, it has been shown that cross-section E (qualified as poor cross-section by operators) has the smallest measured discharge ratio (see figure 3.10).

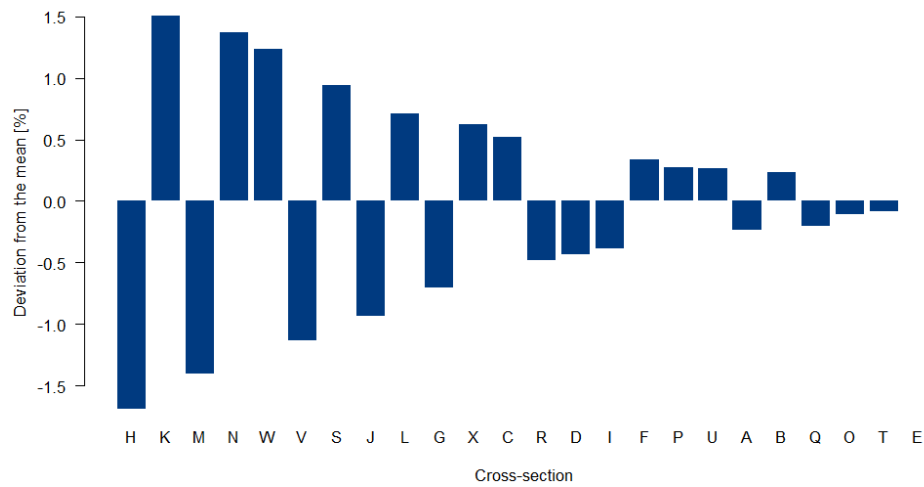


Figure 4.2: Average deviations from the mean of all measurement as a function of the cross-section (sorted in descending order).

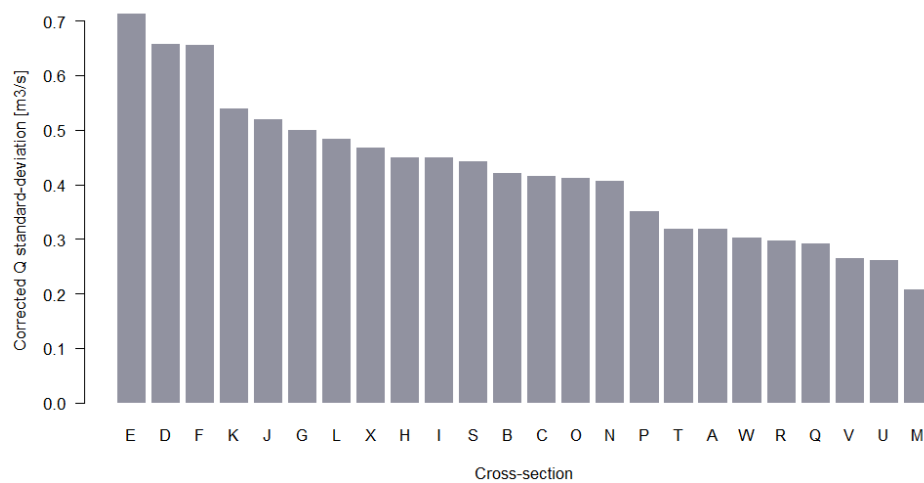


Figure 4.3: Standard-deviation of corrected discharges as a function of the cross-section (sorted in descending order).

## 4.2 Subjective analysis versus objective analysis

Figure 4.4 compares the quality evaluation (percentage of "good" judgment votes) for each cross-section with an objective criteria of dispersion ( $s_x$ , standard-deviation by cross-section) and the bias (average deviation from the mean  $B_x$ ).

There is a direct link between standard-deviation and quality evaluation by operators. Thus, for "poor" cross-sections, the dispersion is higher. However, the bias in terms of discharge (average deviation from the mean), observed for instance at cross-section H, is not correlated with quality evaluation by participants.

It is reminded that QRev post-processing will slightly correct discharge values so that the bias may

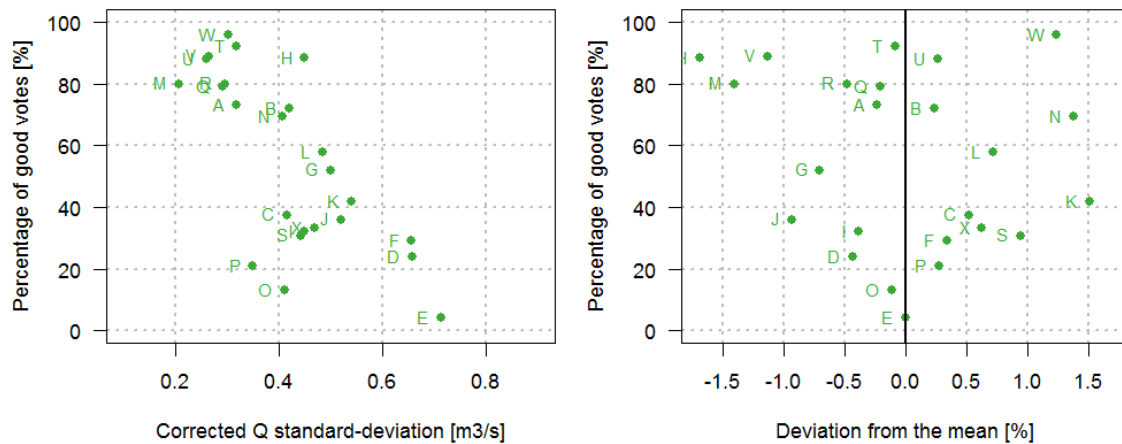


Figure 4.4: Percentage of "good" votes as a function of standard deviation of corrected discharge values (on left) and as a function of average deviation from the mean (on right) for each cross-section.

be reduced.

Similarly, there is no link between measured discharge ratio and quality evaluation as shown on figure 4.5.

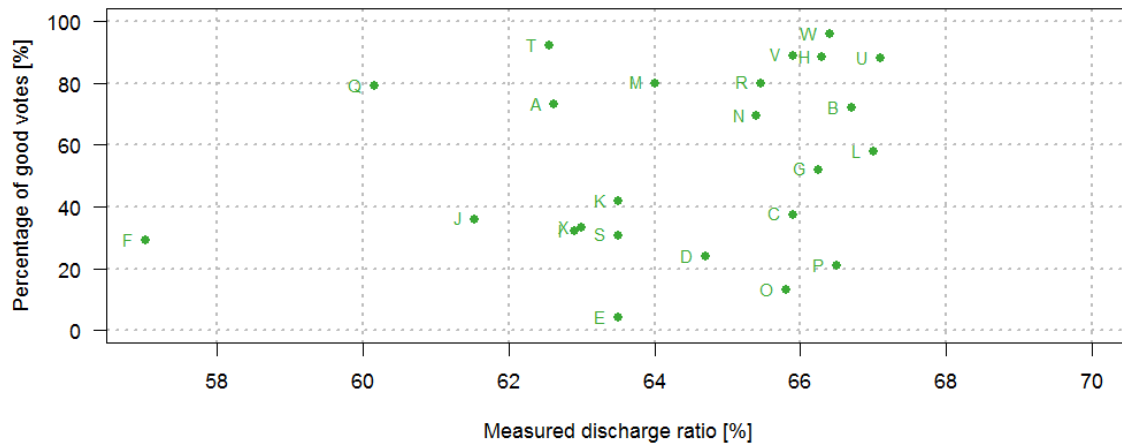


Figure 4.5: Percentage of "good" votes as a function of measured discharge ratio for each cross-section.

### 4.3 Uncertainty based on inter-laboratory experiments

This section is based on computation proposed in Dramais *et al.* (2013), Blanquart (2013) and Le Coz *et al.* (2016). The reader is invited to read appendix G to find detailed explanations to estimate uncertainty based on inter-laboratory experiments. Figure G.1 summarizes the main steps to compute the uncertainty.

### 4.3.1 Results based on corrected discharge estimates

In the context of streamflow measurements, a laboratory is the combination of one or several operator(s) (including extrapolation parameter choices), their equipment (ADCP, software and associated parameters), and their measurement cross-section site. By applying inter-laboratory computations to corrected discharge values all sessions together (equations G.4, G.5, G.7 and G.10 with  $p = 597$  measurements, an averaged number of  $n = 6$  valid transect and  $u(Q_{ref}) = 1\%$ ), the uncertainty estimate is  $\pm 7.3\%$  (at 95% level of confidence, see table 4.1) for a measurement performed with 1 transect in the given measurement conditions of the experiments.

This value is slightly higher than previous inter-laboratory experiments due to less favorable site conditions. The important number of participants lead to a robust uncertainty estimate with a confidence level (again at 95% level of confidence), noted  $U'(U'(Q))$ , between 6.9 and 7.5%.

*Table 4.1: Number of transects, mean discharge, repeatability and interlaboratory standard-deviation, uncertainty and confidence interval (at 95%) in given conditions and for a measurement performed with 6 transects at one of the 24 cross-sections.*

Number of		Mean discharge	$s_r$	$s_L$	$U(Q)$	$U(Q)_{min}-U(Q)_{max}$
measurements	valid transects	$m^3/s$	%	%	%	%
597	3799	14.75	2.1	3.0	$\pm 7.3$	6.9 - 7.5

Figure 4.6 gives the uncertainty (at 95%) of an ADCP measurement as a function of the number of transects and the number of laboratories, according to equation G.15. The expanded uncertainty is estimated to be around  $\pm 6\%$  for a measurement performed with 6 transects in the given measurement conditions of the experiments. The uncertainty is almost the same by averaging discharge over 6 or 10 transects. However, the uncertainty decreases by averaging the measurements performed by two laboratories (different operators, cross-sections and ADCPs). Further research will be conducted to assess which strategy lead to a smaller uncertainty (by using one ADCP at multiple cross-sections? or by using multiple ADCPs at one cross-section?).

Of course, the uncertainty varies among cross-sections as demonstrated by standard-deviation analysis (figure 4.3). Further investigations will be made to estimate the uncertainty due to cross-section effect.

### 4.3.2 Uncertainty estimates according to ADCP models (M9 versus StreamPro)

The inter-laboratory method has been applied to 2 distinct datasets: M9 ADCP (SonTek) discharge measurements and StreamPro ADCP (Teledyne RDI) measurements separately. First results show similar performance between both ADCP models since uncertainty estimates are the same (see table 4.2). Furthermore, since mean discharges are similar (difference  $\ll 1\%$ , it shows the absence of bias between the two manufacturers.



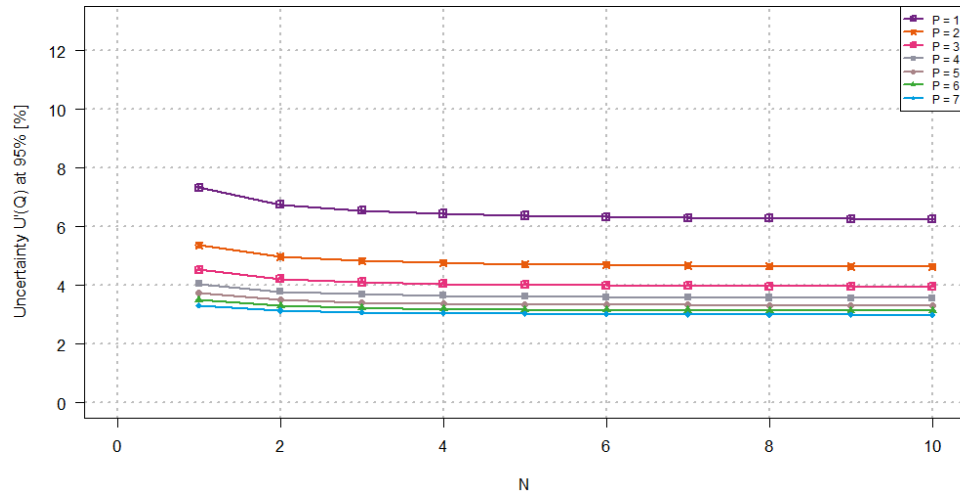
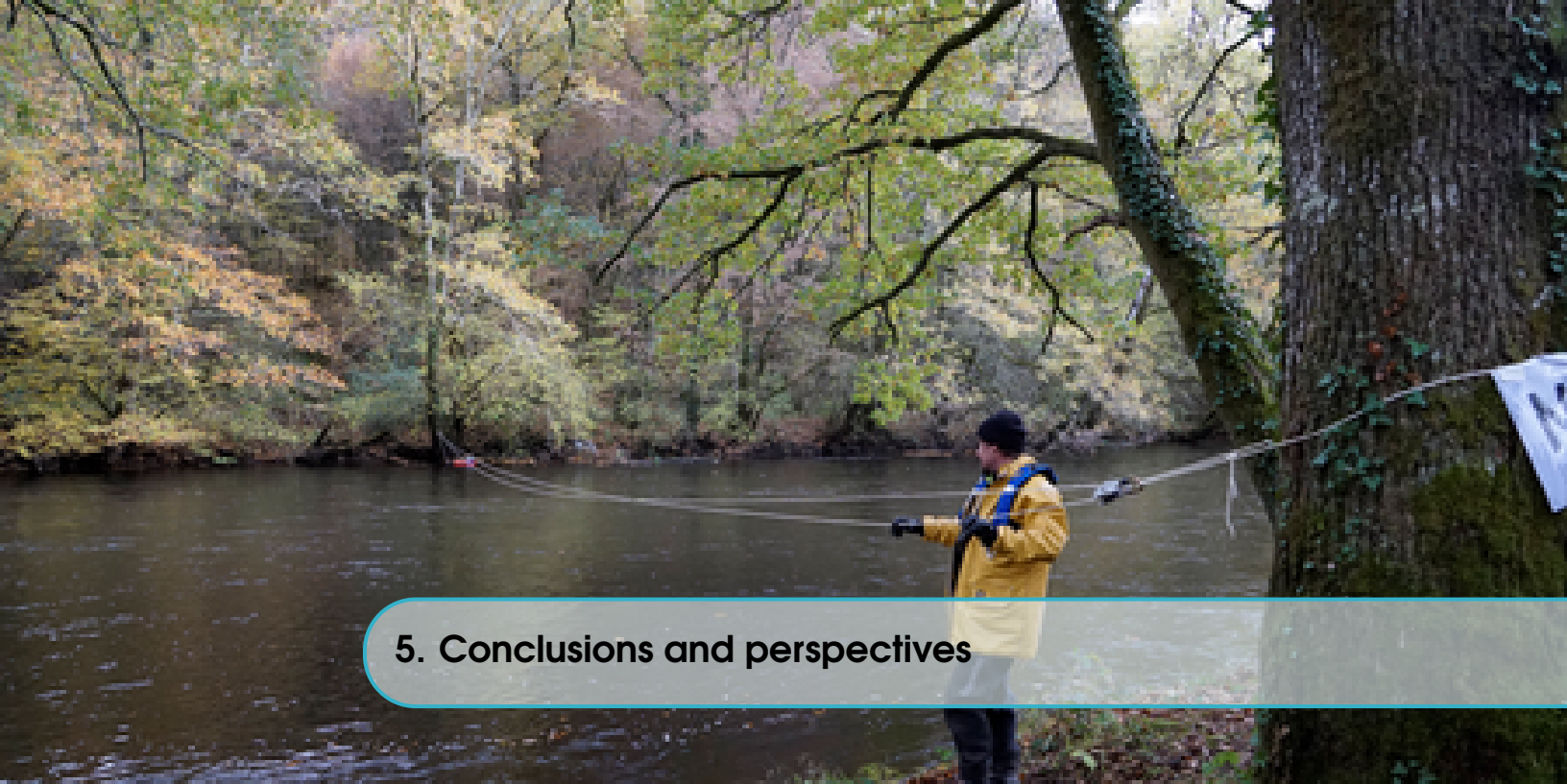


Figure 4.6: uncertainty of a measurement as a function of number  $N$  of transects and number  $p$  of laboratories (at 95% level of confidence). A laboratory is here considered as the combination of several operators, their equipment, and the measurement cross-section site.

Table 4.2: Number of transects, mean discharge, repeatability and interlaboratory standard-deviation, uncertainty and confidence interval (at 95%) associated with M9 and StreamPro ADCP models.

ADCP	Number of		Mean discharge $\text{m}^3/\text{s}$	$s_r$ %	$s_L$ %	$U(Q)$ %	$U(Q)_{\min}-U(Q)_{\max}$ %
	measurements	valid transects					
StreamPro	271	1727	14.81	2.2	2.9	$\pm 7.4$	6.8 - 7.7
M9	227	1451	14.70	1.9	3.0	$\pm 7.2$	6.5 - 7.5



## 5. Conclusions and perspectives

The Chauvan inter-laboratory experiments have proved to be successful (in spite of a complex procedure) in terms of measurements performed (about 600 discharge measurements), participation (50 teams) and technical discussions.

Flow steadiness allowed estimating ADCP discharge uncertainty to be around  $\pm 6\%$  (in given conditions and for a measurement performed with 6 transects at one of the 24 cross-sections) and further investigations will aim at estimating the uncertainty due to cross-section selection.

Additional work will be conducted after post-processing data using QRev software, in cooperation with the USGS. It will allow an homogeneous analysis of ADCP discharge measurements. An analysis will be conducted by comparing default extrapolation coefficients set by operators with automatic or supervised fit of top/bottom discharge extrapolations, as well as comparing Bottom Track reference with GPS mode discharge computations. It may lead to a classification of vertical velocity shapes depending on the cross-section.

Raw data will be further analyzed including the proportion of Bad cells and ensembles, the error velocity, velocities components, the Bottom track quality and the exposure time. The configuration and settings of ADCPs (blinking, the vessel's draft) will be also reviewed.

Then, inter-laboratory uncertainty computations will be post-processed using reviewed discharge measurements. The inter-laboratory method will be also applied on reviewed dataset using various scenarios to investigate the uncertainty due to cross-section effect. For instance, the computations will be applied on discharge measurements from each cross-section leading to 24 uncertainty estimates. These values can be compared with uncertainty based on the whole dataset considering a laboratory as a cross-section (whereas a laboratory was previously considered as the combination of several operators, their equipment, and the measurement cross-section site). This study aims making recommendations regarding deployment strategy to reduce the uncertainty.

Further research will be focused on identifying possible metrics for characterizing the conditions of ADCP discharge measurements related to the uncertainty, especially the uncertainty due to cross-section.

Lastly, inter-laboratory uncertainty estimates will be compared with that provided by propagation computation methods such as OURSIN, developed by CNR (France) (Pierrefeu *et al.*, 2017) ; QRev, by USGS (Oberg et Mueller, 2007) ; QUANT, Environment Canada (Moore *et al.*, 2016) ; QMsys (Muste *et al.*, 2012) , or RiverFlowUA, South Florida Water Management District (González-Castro *et al.*, 2016).

These methods are based on analytic propagation of uncertainties following the Guide to the expression of Uncertainty in Measurement (JCGM, 2008) that allow estimating uncertainty of individual measurement.

The confrontation between inter-laboratory and analytic methods will possibly highlight the best method to compute uncertainty. Otherwise, potential improvements will be identified.



## A. Bonus

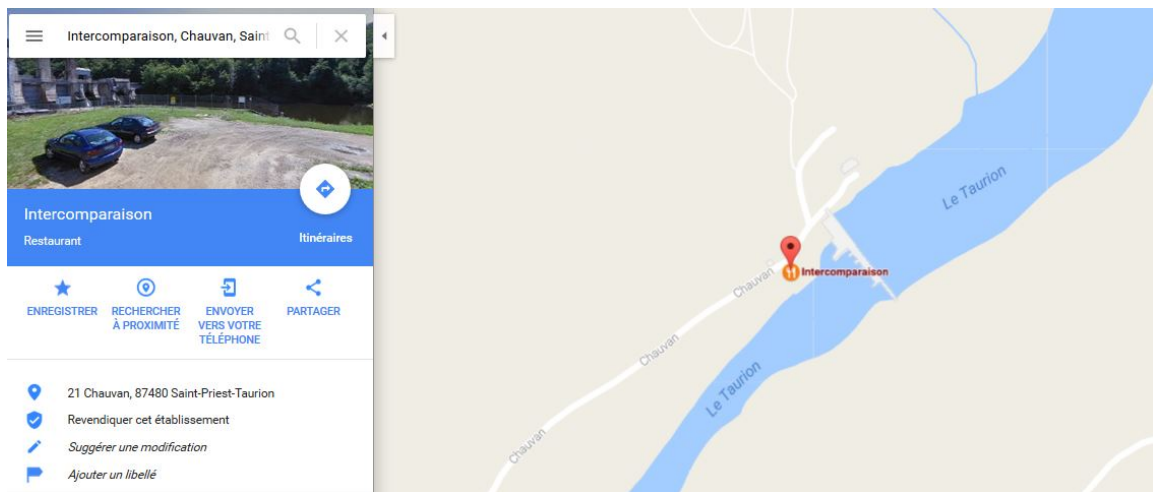


Figure A.1: Since the inter-laboratory experiments, a new restaurant opened, according to Google maps...



*Figure A.2: How to hold a computer during a measurement (prototype).*



*Figure A.3: An umbrella with a window, useful to know when rain is ending.*



Figure A.3: Regional delicacy intercomparison.





**B. Teams**

The following figures show a photograph of team members.



ACAL



ACAL



ANGE



ANGE



AQU1

Figure B.1: Photographs of participants (Source: A. Despax).





AQU2



AQU2



ARA1



ARA2



BRE1



BRE2



CACG

Figure B.1: (... continued) Photographs of participants (Source: A. Despax).



CHA1



CLE2



CHEB



CHA2



CHMC

Figure B.1: (... continued) Photographs of participants (Source: A. Despax).



CHMI



CHP1



CLE1



CNR1

Figure B.1: (... continued) Photographs of participants (Source: A. Despax).



CNR2



CVL1



CVL2



FIXE

Figure B.1: (... continued) Photographs of participants (Source: A. Despax).



ENUK



EPTB



HSM1



IDF1

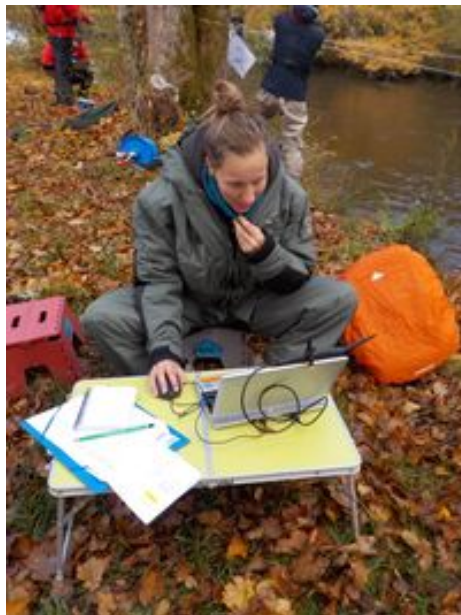
Figure B.1: (... continued) Photographs of participants (Source: A. Despax).



IDF2



IRSA



IRSA



IRSB

Figure B.1: (... continued) Photographs of participants (Source: A. Despax).



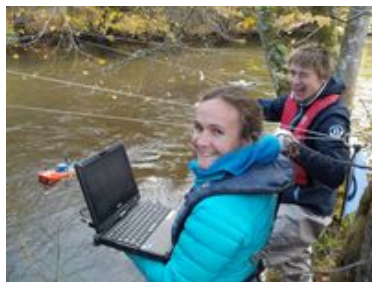
KICT



M2E2



NAN1



IRSL



NAN2



QMEA

Figure B.1: (... continued) Photographs of participants (Source: A. Despax).



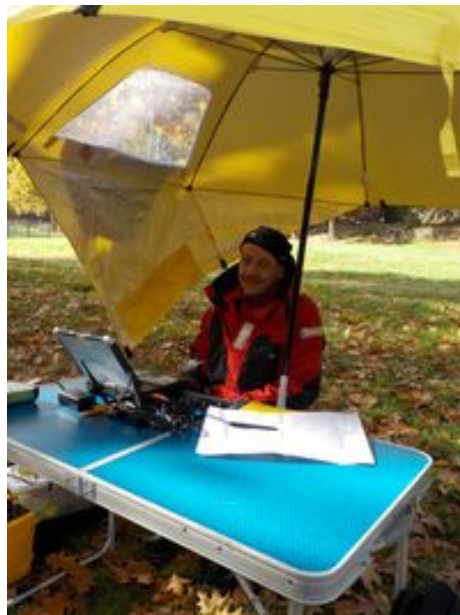
NVE1



PAC1



RED1



RED1

Figure B.1: (... continued) Photographs of participants (Source: A. Despax).





RED2



SMHI



SCP1



SGD1



SGD2

Figure B.1: (... continued) Photographs of participants (Source: A. Despax).



STEK



STEK



TOUR



TRDI



TRDI



TRDI



USGS

Figure B.1: (... continued) Photographs of participants (Source: A. Despax).



VCA1



VCA2



VCA3

Figure B.1: (... continued) Photographs of participants (Source: A. Despax).



*Figure B.2: Members of the coordinating team: from top to bottom and from left to right: David, Alexandre Hauet, Aurélien Despax, Jérôme Le Coz, David Besson, Guillaume Dramais and Arnaud Belleville.*





## C. Cross-sections

### C.1 Upstream-downstream views



Section A - Vue amont



Section A - Downstream view



Section B - Upstream view



Section B - Downstream view

Figure C.1: Upstream and downstream views of each cross-section (Source: A. Hauet).



Section C - Upstream view



Section C - Downstream view



Section D - Upstream view



Section D - Downstream view



Section SCP - Upstream view



Section SCP - Downstream view



Section FIXE - Upstream view



Section FIXE - Downstream view



Section E - Upstream view



Section E - Downstream view

Figure C.1: (...continued) Upstream and downstream views of each cross-section (Source: A. Hauet).



Section F - Upstream view



Section F - Downstream view



Section G - Upstream view



Section G - Downstream view



Section H - Upstream view



Section H - Downstream view



Section I - Upstream view



Section I - Downstream view



Section J - Upstream view



Section J - Downstream view

Figure C.1: (...continued) Upstream and downstream views of each cross-section (Source: A. Hauet).





Section K - Upstream view



Section K - Downstream view



Section L - Upstream view



Section L - Downstream view



Section M - Upstream view



Section M - Downstream view



Section N - Upstream view



Section N - Downstream view



Section O - Upstream view



Section O - Downstream view

Figure C.1: (...continued) Upstream and downstream views of each cross-section (Source: A. Hauet).



Section P - Upstream view



Section P - Downstream view



Section Q - Upstream view



Section Q - Downstream view



Section R - Upstream view



Section R - Downstream view



Section S - Upstream view



Section S - Downstream view



Section T - Upstream view



Section T - Downstream view

Figure C.1: (...continued) Upstream and downstream views of each cross-section (Source: A. Hauet).



Section U - Upstream view



Section U - Downstream view



Section V - Upstream view



Section V - Downstream view



Section W - Upstream view



Section W - Downstream view



Section X - Upstream view



Section X - Downstream view

Figure C.1: (...continued) Upstream and downstream views of each cross-section (Source: A. Hauet).

C.2 Cross-section characteristics

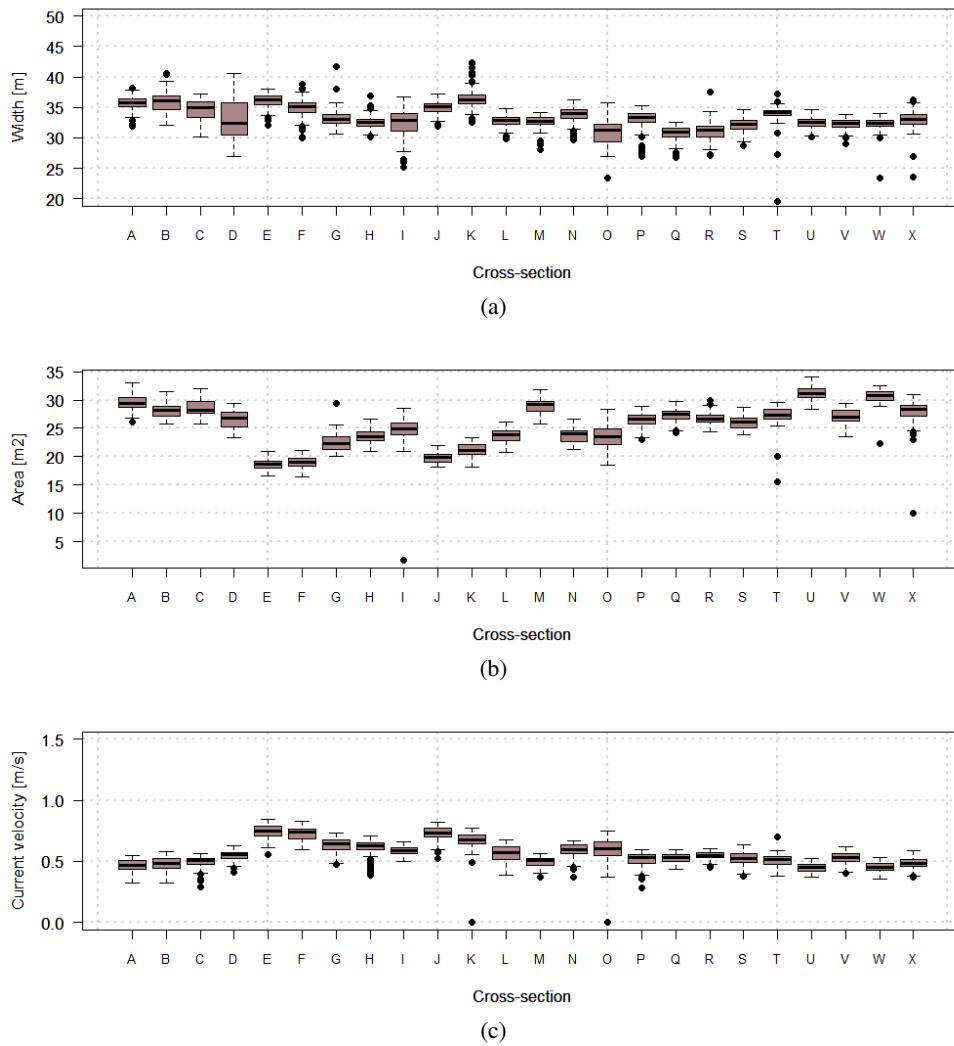


Figure C.2: Distributions of widths, areas and current velocities of the 24 cross-sections.





## D. Procedure

### D.1 Incident sheets

Intercomparaison GDH - Chauvan 2016  
Fiche de suivi en berge

Opérateur en berge : David Besson  
Secteur : R-R

Date / Heure début	Heure de fin	Transect	Equipe	Type d'incident	Conséquence
8/11/16	13h52	M	22	flissing samples	recuperation fichier Tête ADCP à posteriori
8/11/16 13h53	14h12	J	24	" "	fichier recover OK!
8/11/16	14h47	M	24	" "	Pb batterie 14h58 + recuperation données à faire
8/11/16 15h34	15h50	O	37	pb batterie	recuperation faite OK pas de pb
8/11/16 17h30	17h40	O	organisateur	chgt profils décalé 2m en avant R.Mont	
9/11/16 8h30	8h50	TWXS		chgt ADCP (SP) dès le	début de la manipulation (4 heures de nuit)
9/11/16 15h30	16h35	O	16	5 profils / 6 valide	Requis completé ultérieurement 2 fichiers de résultats OK
8/11 13h	13h52	M	22	flissing samples	recuperation fichier dans la tête ADCP à posteriori OK
8/11 13h53	14h12	J	24	" "	fichier recover/recuperer OK
8/11	14h47	M	24	" "	problème batterie 14h58 recuperation données à faire
8/11 15h34	15h50	O	37	problème batterie	recuperation faite OK pas de problème
8/11 17h30	17h40	O	organisateur	changement profils. décalé 2m en avant en R.Mont	
9/11 8h30	8h50	TWXS	12	changement ADCP (SP) dès le	début de la manipulation (5h)
9/11 15h30	16h35	O	16	5 profils / 6 valide	Requis completé ultérieurement 2 fichiers de résultats OK

Figure D.1: Incident sheet example (in French).

D.2 Road map

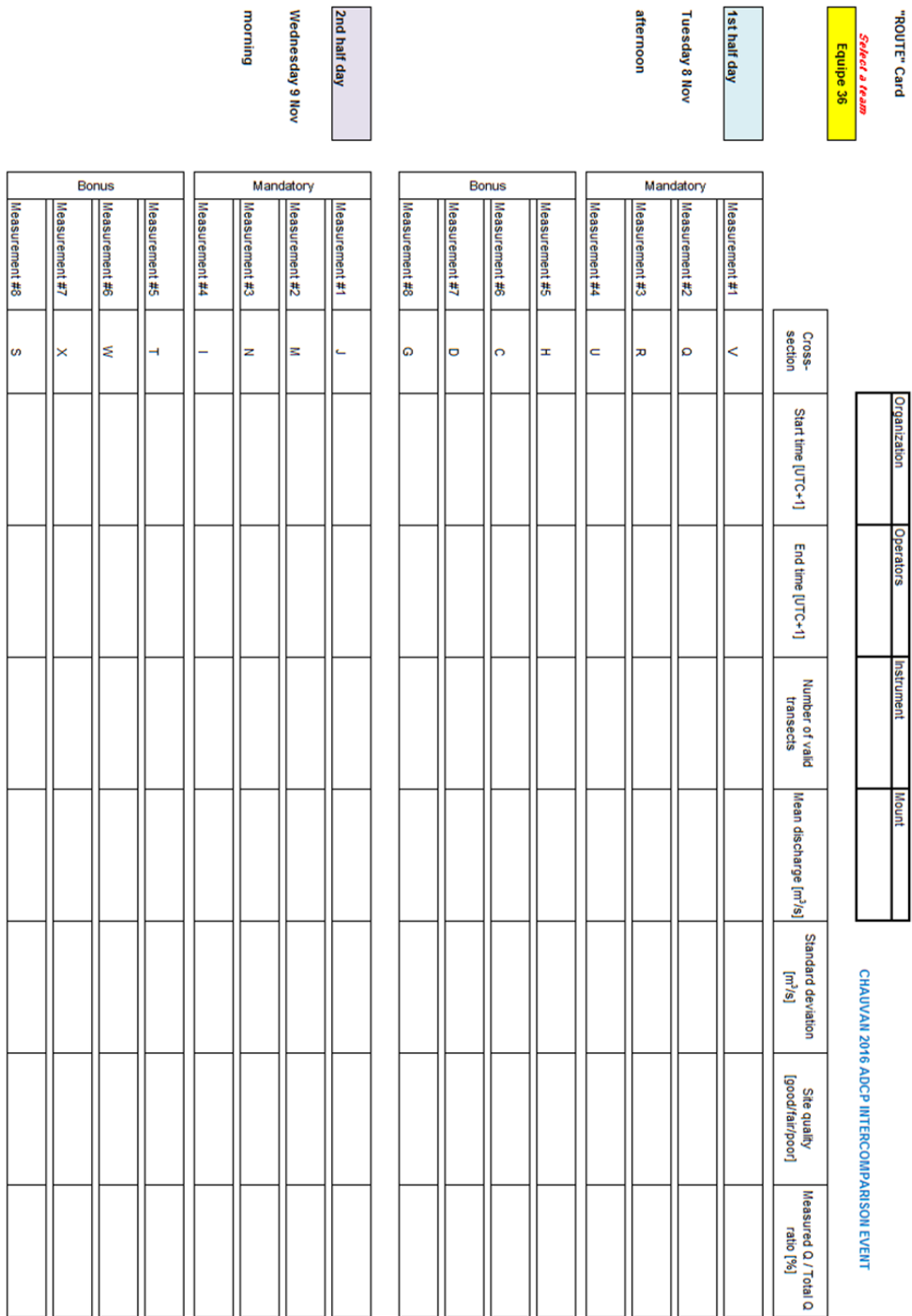
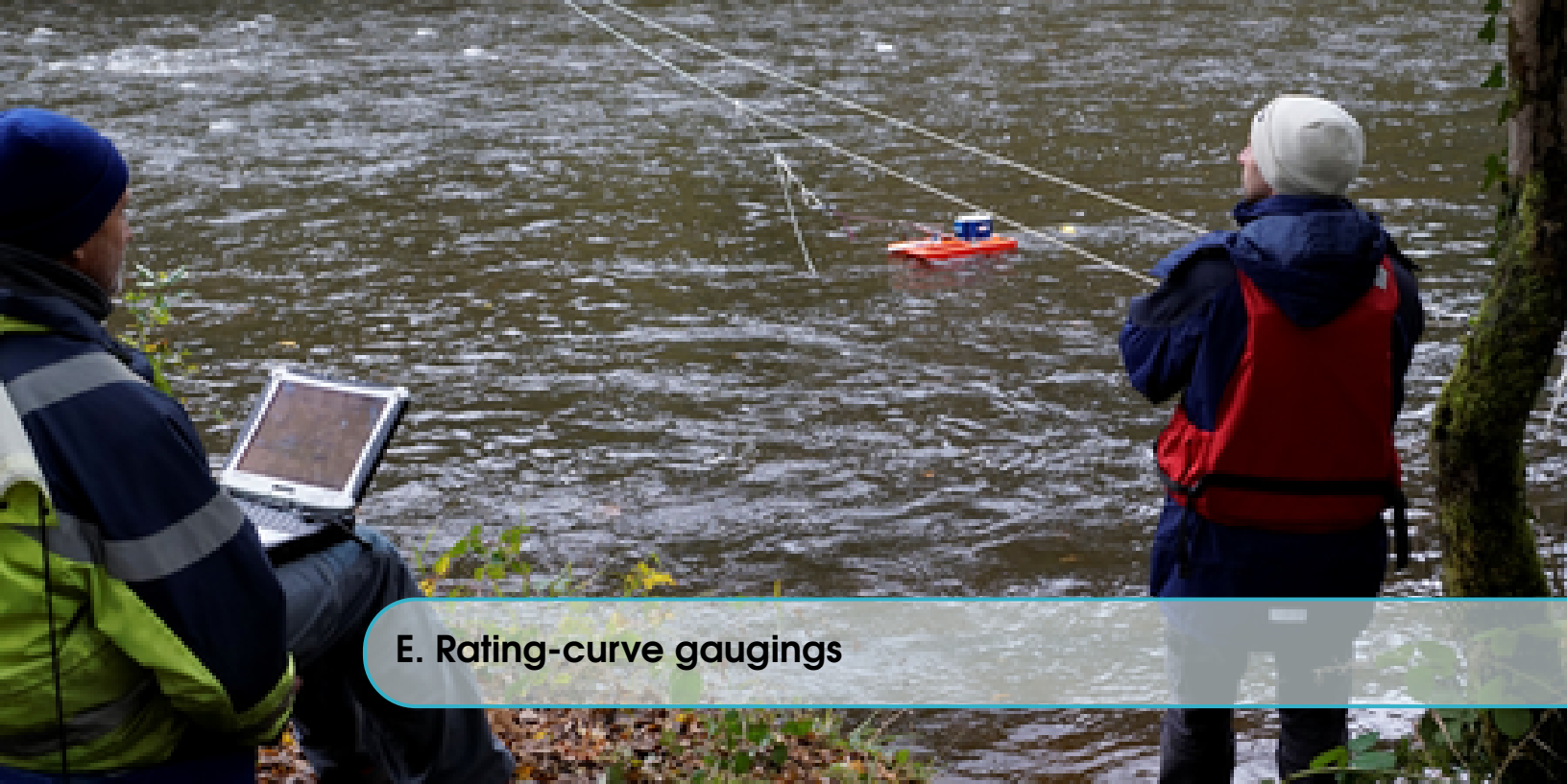


Figure D.2: Road map example.



## E. Rating-curve gaugings

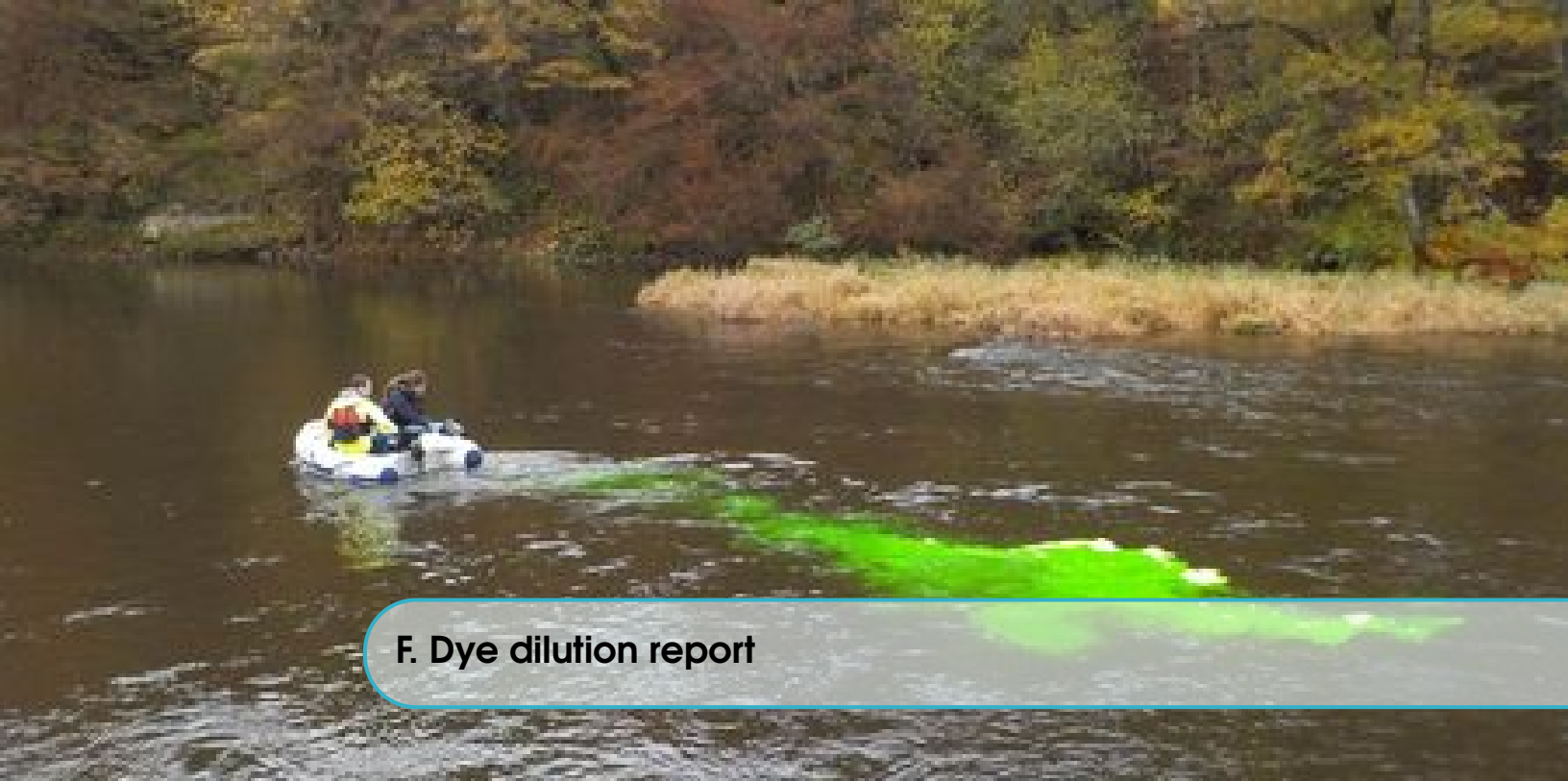
The following table E.1 present all the gaugings used to plot the stage-dischare relationship (see section 3.2). All gaugings were performed using StreamPro ADCPs exceptd the measurements number 103 (current-meter on wading rods), number 108 (not documented) and number 120 (RiverRay ADCP model).

Since 2015, all the ADCP gaugings were performed on cross-section labeled FIXE upstream of the weir (see 2.5). Before 2013, some gaugings were performed from a bridge 2.5 km downstream of the EDF-DTG hydrometric station.



Table E.1: Gaugings performed at EDF-DTG hydrometric station since 2008. SP, RR and MP mean StreamPro ADCP, RiverRay ADCP and current-meter measurement. NONDTG measurement is not documented.

Number	Water level m	Discharge m <sup>3</sup> /s	Date DD/MM/YYYY	Method
82	0.76	15.7	18/03/2008	SP
83	0.32	2.82	19/05/2008	SP
84	0.43	4.84	19/05/2008	SP
85	0.645	9.57	19/05/2008	SP
86	0.925	17.4	20/05/2008	SP
87	1.07	26.6	20/05/2008	SP
88	0.54	6.63	22/07/2008	SP
89	0.8	13.8	23/12/2008	SP
90	0.6	8.25	09/07/2009	SP
91	0.32	2.76	17/11/2009	SP
92	1.09	28	17/02/2010	SP
93	1.125	30.3	02/06/2010	SP
94	1.14	32.3	07/12/2010	SP
95	0.57	7.53	09/02/2011	SP
96	0.585	8.09	29/06/2011	SP
97	0.32	2.62	13/07/2011	SP
98	0.31	2.42	29/09/2011	SP
99	0.83	15.1	17/01/2012	SP
100	1.06	26.4	13/03/2012	SP
101	0.93	18.2	10/04/2012	SP
102	0.325	2.85	05/06/2012	SP
103	0.33	2.74	31/07/2012	MP
104	0.74	12.2	28/08/2012	SP
105	0.33	2.74	25/09/2012	SP
106	0.31	2.47	23/10/2012	SP
107	0.61	8.61	20/11/2012	SP
108	1.59	75.6	06/02/2013	NONDTG
109	1.285	47	19/02/2013	SP
110	0.96	19.7	14/05/2013	SP
111	0.45	4.95	08/10/2013	SP
112	1.29	46.99	05/02/2014	SP
113	1.29	50.1	20/02/2014	SP
114	0.33	2.52	10/09/2014	SP
115	0.835	15.1	18/11/2014	SP
116	1.14	31.8	12/02/2015	SP
117	1.13	31.5	24/03/2015	SP
118	0.64	8.76	18/06/2015	SP
119	0.49	6.1	30/06/2015	SP
120	1.33	54	24/02/2016	RR
121	1.285	46.2	07/06/2016	SP
122	0.38	3.74	08/09/2016	SP



**F. Dye dilution report**

## Mesure de débit

### Station

ID	chauvan	Commentaire
Emplacement	intercomparaison	
Site	stade	

### Mesure

Date/Heure	09/11/2016	Commentaire: Long car stockage temporaire dans le remous en aval du barrage.
Opérateurs	bouchet cordeau	
Quantité Traceur	18 g	
Site d'injection	vanne barrage	
Distance de dissolution	800 m	
Niveau d'eau	0 cm	

### Débit

	Débit [l/s]	Dév. [%]	Base [mV]	Max. [mV]	□
A	14376	3.0	44.5-44.7	81.6	
B	13325	-4.5	43.8-43.9	122.3	
CA	13877	-0.5	46.8-46.3	137.2	
CB	14235	2.0	47.1-48	94.5	
Moyenne [l/s]	13953				

### Calibration

Date/Heure	08/11/2016	09:37:41		
	Coefficient	Corrélation	Base [mV]	
A	0.028926	0.9999	54.1	
B	0.028141	0.9999	53.0	
CA	0.027054	0.9999	53.7	
CB	0.026972	0.9999	55.7	

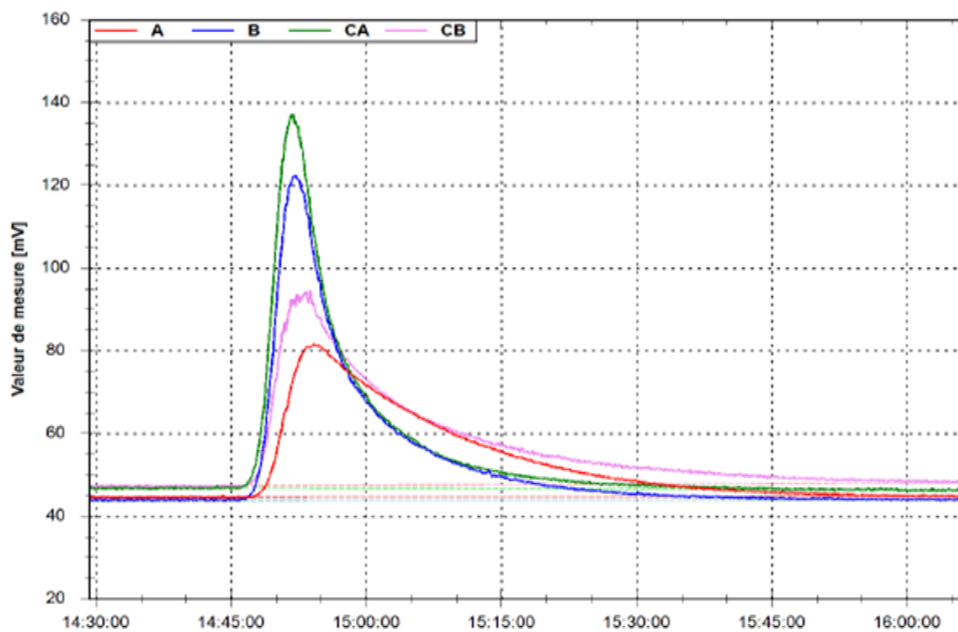


Figure F.1: Dye dilution gauging report (in French).



## G. Principles and computations for estimating uncertainty

The following explanations are extracted from and based on Le Coz *et al.* (2016) paper.

Interlaboratory experiments are a useful method to estimate uncertainty when a mathematical model of the whole measurement process is not available, or too complex. In essence, interlaboratory experiments consist of measuring the same variable (or measurand) with several participants 'or laboratories' using the same measurement procedure. In the context of streamflow measurements, a 'laboratory' is the combination of one or several operator(s), their equipment and their measurement site. Note that 'laboratory' does not mean 'facility' here: in the field of hydrometry all the laboratories must work in the same facility, i.e. stream section, since the single flow that has to be measured by all participants cannot be transferred in time and space.

The data processing follows the guidelines provided by the following international standards:

- ISO (1994b): quantification of the performance of a measurement technique in terms of repeatability and reproducibility;
- ISO (2005): translation of previous results in terms of measurement uncertainty;
- ISO (2010): determination of the uncertainty associated with the average flow rate calculated from all participants;
- ISO (1994a): determination of the uncertainty associated with the repeatability and reproducibility estimates.

Several assumptions are necessary for the implementation of these standards. First, only the error sources covered by the tests are considered as included in the experimental results. Also, it is assumed that the results are uncorrelated and that the measurement errors follow a Gaussian (or at least unimodal) distribution. Last, in the ISO (1994b) standard, it is assumed that the repeatability is the same for all participants, and to a lesser extent, that the number of runs is the same for all participants.

### Model of error

Consider  $Q_{i,k}$ , the  $k^{\text{th}}$  instantaneous discharge measurement performed by the  $i^{\text{th}}$  laboratory during a steady flow:

$$Q_{i,k} = Q_{\text{true}} + \delta + B_i + \varepsilon_{i,k} \quad (\text{G.1})$$

with  $Q_{\text{true}}$  the true discharge value (unknown),  $\delta$  the bias associated with the measurement technique (the same for all participants involved in the interlaboratory experiment), and  $B_i$  and  $\varepsilon_{i,k}$  the systematic (bias) and random errors related to the  $i^{\text{th}}$  laboratory and its  $k^{\text{th}}$  measurement.

During an interlaboratory experiment, the reference discharge value is built as  $Q_{\text{mean}} = Q_{\text{true}} + \delta$ , the average of all discharge values of the experiment, i.e. of all the measurements obtained by all the  $p$  laboratories involved in the experiment.

The measurement errors in the  $k^{\text{th}}$  discharge  $Q_{i,k}$  measured by the  $i^{\text{th}}$  laboratory can be modelled as follows:

$$Q_{i,k} = Q_{\text{mean}} + B_i + \varepsilon_{i,k} \quad \text{with} \quad B_i \sim \mathcal{N}(0, \sigma_L) \quad \text{and} \quad \varepsilon_{i,k} \sim \mathcal{N}(0, \sigma_r) \quad (\text{G.2})$$

The random error,  $\varepsilon_{i,k}$ , is assumed to follow a Gaussian distribution of mean zero and standard deviation  $\sigma_r$ . With the needed corrections being applied to results, the systematic error,  $B_i$ , is assumed to follow a Gaussian distribution of mean zero and standard deviation  $\sigma_L$ . This assumption requires that instruments are calibrated and corrected at the maximum extent possible.

ISO (2005) is based on the following uncertainty propagation equation, which allows for uncertainty budgets in compliance with the GUM:

$$u^2(y) = u^2(\hat{\delta}) + s_L^2 + \sum c_i^2 u^2(x_i) + s_r^2 \quad (\text{G.3})$$

where  $u(y)$  is the uncertainty associated with the measurement result ( $y$ ),  $u(\hat{\delta})$  is the uncertainty associated with the estimator of the measurement technique bias ( $\hat{\delta}$ ),  $s_L$  is the interlaboratory standard deviation,  $u(x_i)$  with sensitivity coefficients  $c_i$  are the uncertainties related to the effects not covered in the experiments (input quantities  $x_i$ ), and  $s_r$  is the intra-laboratory standard deviation (repeatability). In order not to double count errors or miss some of them in applying Eq. G.3, it is important to associate every elemental error sources with covered or not covered effects.

## G.1 Processing of the comparison results

The processing of results obtained from interlaboratory experiments is detailed in the ISO (1994b) standard. After collecting and formatting the data, the reviewing of the individual measurement values is carried out. The ISO (1994b) standard recommends that  $h$  and  $k$  Mandel criteria be calculated and plotted, in order to visually check the homogeneity and consistency of the measurements. These criteria intend to quickly identify participants that would present a different behaviour, in terms of accuracy ( $h$  criteria) or in terms of dispersion ( $k$  criteria). Detecting one or several participants with a markedly different behaviour compared to others may lead to statistical tests for outlier detection, with the optional implementation of Cochran and Grubbs tests. Such tests may be used to justify discarding data from the pool, in order to get a homogeneous sample that is representative of the performance of instruments and participants with similar accuracy and dispersion. The reader is referred to the ISO (1994b) standard for precise details on how to implement  $h$  and  $k$  Mandel criteria, as well as Cochran and Grubbs tests.

ISO (1994b) standard provides procedures for computing the variance estimators,  $s_r$ ,  $s_L$  and  $s_R$  in Eq. G.3, using the results of the interlaboratory experiments. Such estimators respectively provide the best estimates of the true repeatability, interlaboratory and reproducibility standard deviations,  $\sigma_r$ ,  $\sigma_L$  and  $\sigma_R$ , which remain unknown.

The repeatability  $s_r$  is computed from the experimental standard deviations,  $s_i$ , of the  $n_i$  repeated discharge measurement,  $Q_{i,k}$ , provided by each participant  $i$ , as follows:

$$s_r^2 = \frac{\sum_{i=1}^p (n_i - 1) s_i^2}{\sum_{i=1}^p (n_i - 1)} \quad \text{with} \quad s_i^2 = \frac{1}{n_i - 1} \sum_{k=1}^{n_i} (Q_{i,k} - \bar{Q}_i)^2 \quad (\text{G.4})$$

In case  $n_i = 2$  only, the standard deviation is estimated to be  $s_i = |Q_{i,2} - Q_{i,1}|/\sqrt{2}$ .

The interlaboratory standard deviation,  $s_L$ , is estimated using the following equation:

$$s_L^2 = \frac{s_d^2 - s_r^2}{\bar{n}} \quad \text{with} \quad s_d^2 = \frac{1}{p-1} \sum_{i=1}^p n_i (\bar{Q}_i - Q_{\text{mean}})^2 \quad \text{and} \quad \bar{n} = \frac{1}{p-1} \left[ \sum_{i=1}^p n_i - \frac{\sum_{i=1}^p n_i^2}{\sum_{i=1}^p n_i} \right] \quad (\text{G.5})$$

In case that  $s_d < s_r$ ,  $s_L$  is taken equal to zero.

Then, the reproducibility standard deviation,  $s_R$ , is simply taken to be equal to:

$$s_R^2 = s_r^2 + s_L^2 \quad (\text{G.6})$$

ISO (2005) is finally invoked to assimilate  $s_R$  and  $u(Q)$ , the combined standard uncertainty of the discharge. Assuming that all the non-negligible error sources were covered through the interlaboratory experiments, then the  $c_i u(x_i)$  terms can be neglected and Eq. G.3 from ISO (2005) leads to the following expression of the expanded discharge uncertainty:

$$U(Q) = k \sqrt{s_R^2 + u^2(\hat{\delta})} = k \sqrt{s_r^2 + s_L^2 + u^2(\hat{\delta})} \quad (\text{G.7})$$

with  $k$  the coverage factor used to expand the uncertainty within a given probability level. The Hydrometric Uncertainty Guidance (HUG) (ISO, 2007) recommends that  $k = 2$  should be chosen because the corresponding 95% probability level is considered to be the most appropriate for many testing and calibration applications. In this whole document, uncertainty components  $u(X)$  are relative standard uncertainties (in % of measurand  $X$ ), while terms  $U(X)$  denote the relative expanded uncertainties ( $U(X) = k u(X)$ ,  $k = 2$ , 95% probability level). Also remind that the standard uncertainty,  $u(\hat{\delta})$ , is related to the estimation of the streamgauging technique bias,  $\hat{\delta}$ , which is discussed in the next section.

## G.2 Estimation of the streamgauging technique bias

Estimation of the discharge measurement technique bias,  $\hat{\delta}$ , and its uncertainty,  $u(\hat{\delta})$ , is not a trivial task when no reference value is available, which is almost always the case for stream discharges in natural conditions. Ideally, a reference value should be a reproducible value with a widely accepted,

small uncertainty, and related to the most fundamental international standards. The most accurate determination of a discharge (in m<sup>3</sup>/s) would be the measurement of the water volume difference (in m<sup>3</sup>) over a given duration (in seconds), or the measurement of its weight and density. Such an accurate reference measurement is feasible in small scale laboratory conditions, but obviously not in natural streams.

Alternatively, a GUM-based approach could be followed in order to propagate the elemental uncertainties related to the measurement technique bias, based on available laboratory calibrations traceable to metrological standards. For instance, the bias in measuring the water velocity and the bottom-track velocity by current-meters and acoustic profilers (ADCP) can be assessed from testing in tow-tank facilities. Unfortunately, this approach cannot be completed for all the systematic errors of discharge measurements in natural conditions, because of the large number of elemental error sources and the complexity of those related to the environment and the operator effects.

In best cases, it is possible to compare the average result,  $Q_{\text{mean}}$ , of all the participants of an interlaboratory experiment with some reference discharge value,  $Q_{\text{ref}}$ , given by another system with a quantified and smaller uncertainty,  $u(Q_{\text{ref}})$ . Then, the expressions for  $\hat{\delta}$  and  $u(\hat{\delta})$  simply write:

$$\hat{\delta} = Q_{\text{mean}} - Q_{\text{ref}} \quad (\text{G.8})$$

$$u^2(\hat{\delta}) = u^2(Q_{\text{mean}}) + u^2(Q_{\text{ref}}) \quad (\text{G.9})$$

The latter equation (Eq. G.8) assumes that the measurement errors of the tested streamgauging technique and the reference are statistically independent. Note that Eq. G.8 for  $u(\hat{\delta})$  is preferred over the estimation proposed in Section 6.3.3.1 of ISO (1994a) where the uncertainty of the reference discharge is neglected, which is not valid in hydrometric applications.

According to the Eq. 15 of ISO (2005) standard, the uncertainty in  $Q_{\text{mean}}$  can be evaluated considering the number,  $n$ , of measurements repeated by each of the  $p$  participants during the experiment, which leads to the following equation:

$$u(\hat{\delta}) = \sqrt{\frac{s_r^2}{np} + \frac{s_L^2}{p} + u^2(Q_{\text{ref}})} \quad (\text{G.10})$$

Note. Even using a reliable and precise reference measuring system, many interlaboratory experiments are necessary to assess  $\hat{\delta}$ ,  $u(\hat{\delta})$  and their possible dependencies on major influence factors. Usually, a major practical issue is to assess  $u(Q_{\text{ref}})$ , which must be estimated independently of the interlaboratory experiments, of course.

### G.3 Uncertainty of the uncertainty estimates

Due to the limited number,  $p$  and  $n$ , of participants and repeated measurements, respectively, there is some uncertainty in the results of the interlaboratory experiments due to the sampling variability. The ISO (1994a) standard introduces the following approximate equations for assessing the relative uncertainty of  $s_r$  and  $s_R$  estimates with a probability level of 95%:

$$A_r = 1.96 \sqrt{\frac{1}{2p(n-1)}} \quad (\text{G.11})$$

$$A_R = 1.96 \sqrt{\frac{p[1 + n(\gamma^2 - 1)]^2 + (n-1)(p-1)}{2\gamma^4 n^2 (p-1)p}} \quad (\text{G.12})$$

where  $\gamma = \sigma_R / \sigma_r \approx s_R / s_r$ .

Neglecting the streamgauging technique bias,  $u(\hat{\delta})$ , in Eq. G.7, means that the 'true' uncertainty,  $2\sigma_R$ , is estimated by  $U(Q) = 2s_R$ , i.e. twice the reproducibility standard deviation. Re-arranging Eq. 7 of ISO (1994a), which states that  $(s_R - \sigma_R) / \sigma_R \in ] -A_R; A_R[$ , leads to the following uncertainty interval around the 'true' discharge uncertainty:

$$\frac{U(Q)}{1 + A_R} < 2\sigma_R < \frac{U(Q)}{1 - A_R} \quad (\text{G.13})$$

or:

$$2\sigma_R(1 + A_R) < U(Q) < 2\sigma_R(1 - A_R) \quad (\text{G.14})$$

It is helpful for assessing the relative advantage of increasing the number of repeated discharge measurements,  $n$  or the number of laboratories,  $p$  to improve the accuracy of the reproducibility estimate, hence of the uncertainty estimate,  $U(Q)$ .

## G.4 Averaged discharge measurements

In some streamgauging techniques, each discharge measurement,  $Q^{N,P}$ , is actually established from the average of  $N$  repeated measurements for each of  $P$  instruments. For example, a gauging conducted with an ADCP is usually the mean of  $N = 4 - 6$  successive transects. Usually,  $P = 1$ , but for specific applications when a minimal uncertainty is required, several ADCP may be used simultaneously and their results may be averaged altogether.

Using interlaboratory experiments data for ADCP gaugings, it is possible to compute the uncertainty on  $Q^{N,P}$  'directly', by applying the interlaboratory procedure to discharge data established as in the field, i.e. as the average of  $N \times P$  primary discharge measurements from  $N$  successive transects and  $P$  ADCP. However, computing  $s_r$  and  $s_R$  from discharge data established from each ADCP transect is more convenient because individual discharges do not have to be clustered by 4 or 6. The uncertainty estimation is also expected to be more accurate, since Eq. G.11 and Eq. G.12 show that  $A_r$  and  $A_R$  are smaller when  $n$  and  $p$  are greater. The ISO (2005) standard can again be followed to establish the following formula to extend the uncertainty results obtained from elementary discharges (1 transect, 1 ADCP) to the uncertainty in discharge values determined as the average of  $N$  successive measurements done by each of  $P$  instruments:

$$U(Q^{N,P}) = k \sqrt{\frac{s_r^2}{NP} + \frac{s_L^2}{P} + u^2(\hat{\delta})} \quad (\text{G.15})$$

In recurrent cases when there is a significant directional bias in the ADCP measurements, i.e. between transects conducted in opposite directions, it would be better to compute  $s_r$  and  $s_R$  from discharge averaged over a pair of opposite transects. This would avoid overestimating the repeatability variance since ADCP gaugings are usually the average of a number of transect pairs.



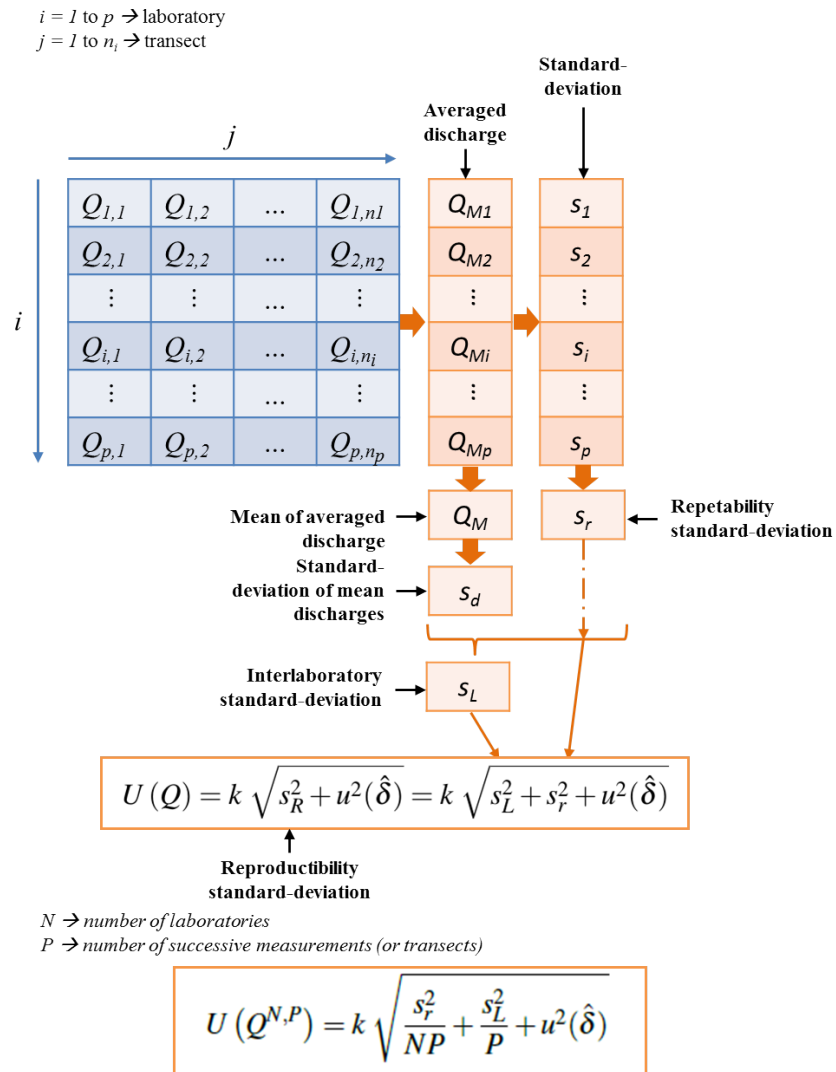


Figure G.1: The main steps to compute the inter-laboratory uncertainty.



## Bibliography

- ATMANE, D. (2012). Les essais interlaboratoires en hydrométrie : analyse des campagnes de mesures réalisées et amélioration du protocole. Mémoire de fin d'études. université de nancy.
- BLANQUART, B. (2013). Panorama des méthodes d'estimation des incertitudes de mesure. *La Houille Blanche*, 6:9–15.
- DESPAX, A., DRAMAIS, G. et HAUET, A. (2014). Comparaison de mesures du débit des petits cours d'eau par courantomètres sur perche. Journées d'intercomparaison des 15, 16 et 17 octobre 2013. Rapport d'essais, Groupe Doppler. 54 p.
- DESPAX, A., FAVRE, A.-C., BELLEVILLE, A., HAUET, A., LE COZ, J., DRAMAIS, G. et BLANQUART, B. (2016). Field inter-laboratory experiments versus propagation methods for quantifying uncertainty in discharge measurements using the velocity-area method. *In Proceedings of River Flow 2016, Saint-Louis, USA*. 7 p.
- DRAMAIS, G., BLANQUART, B. et LE COZ, J. (2011). Comparaison de méthodes de mesure du débit des petits cours d'eau. Journées d'intercomparaison des 17 et 18 mai 2011. Rapport d'essais. 53 p.
- DRAMAIS, G., BLANQUART, B., LE COZ, J., PIERREFEU, G., HAUET, A., ATMANE, D. et POBANZ, K. (2013). Les essais interlaboratoires en hydrométrie : méthodologie et cas d'applications. *SHF, Colloque Hydrométrie 2013, Paris*. 10 p.
- EVERARD, N. (2007). ADCP Regatta (2007) River Severn at Bewdley 21st August 2007. Rapport d'essais, UK Environment Agency. 12 p.
- EVERARD, N. (2009). ADCP Regatta (2009) River Severn at Bewdley 4th June 2009. Rapport d'essais, UK Environment Agency. 30 p.
- GONZÁLEZ-CASTRO, J., BUZARD, J. et MOHAMED, A. (2016). Riverflowua—a package to estimate total uncertainty in adcp discharge measurements by fotse—with an application in hydrometry. *In River Flow 2016*, pages 715–723. CRC Press.

- HAUET, A., LE COZ, J., SEVREZ, D., DRAMAIS, G., HÉNAULT, F., PERRET, C., PIERREFEU, G., POBANZ, K. et THOLLET, F. (2012). Intercomparaison ADCP sur le canal de La Gentille (12-16/09/2011). [adcp intercomparison in the gentille canal (2011/09/12-16). Rapport d'essais, Groupe Doppler. 62 p.
- ISO (1994a). ISO 5725-1:1994 - Exactitude (justesse et fidélité) des résultats et méthodes de mesure – Partie 1: Principes généraux et définitions. 29 p.
- ISO (1994b). ISO 5725-2:1994 - Exactitude (justesse et fidélité) des résultats et méthodes de mesure – Partie 2: Méthode de base pour la détermination de la répétabilité et de la reproductibilité d'une méthode de mesure normalisée. 55 p.
- ISO (2005). ISO 13528:2005 - Statistical methods for use in proficiency testing by interlaboratory comparisons. 66 p.
- ISO (2007). ISO/TS 25377:2007 - Hydrometry – Hydrometric Uncertainty Guidance (HUG). 59 p.
- ISO (2010). ISO 21748:2010 - Lignes directrices relatives à l'utilisation d'estimations de la répétabilité, de la reproductibilité et de la justesse dans l'évaluation de l'incertitude de mesure. 38 p.
- JCGM (2008). Evaluation of measurement data - Guide to the expression of uncertainty in measurement. Guide 100, BIPM. 132 p.
- LE COZ, J., BLANQUART, B., POBANZ, K., DRAMAIS, G., PIERREFEU, G., HAUET, A. et DESPAX, A. (2016). Estimating the uncertainty of streamgauging techniques using in situ collaborative interlaboratory experiments. *Journal of Hydraulic Engineering*, 7(142):04016011.
- LE COZ, J., RENARD, B., BONNIFAIT, L., BRANGER, F. et LE BOURSICAUD, R. (2014). Combining hydraulic knowledge and uncertain gaugings in the estimation of hydrometric rating curves: A Bayesian approach. *Journal of Hydrology*, 509:573–587.
- LE COZ, J., SAYSSET, G. et PIERREFEU, G. (2009). Régate ADCP Vézère 2009. Rapport d'essais, Groupe Doppler. 14 p.
- MOORE, S. A., JAMIESON, E. C., RAINVILLE, F., RENNIE, C. D. et MUELLER, D. S. (2016). Monte carlo approach for uncertainty analysis of acoustic doppler current profiler discharge measurement by moving boat. *Journal of Hydraulic Engineering*, page 04016088.
- MORLOT, T. (2014). *La gestion dynamique des relations hauteur-débit des stations d'hydrométrie et le calcul des incertitudes associées. Un indicateur de gestion, de qualité et de suivi des points de mesure*. Thèse de doctorat, Université de Grenoble, Grenoble. 293 p.
- MORLOT, T., PERRET, C., FAVRE, A.-C. et JALBERT, J. (2014). Dynamic rating curve assessment for hydrometric stations and computation of the associated uncertainties: Quality and station management indicators. *Journal of Hydrology*, 517:173–186.
- MUELLER, D. S. (2013). extrap: Software to assist the selection of extrapolation methods for moving-boat adcp streamflow measurements. *Computers & Geosciences*, 54:211–218.

- 
- MUELLER, D. S. (2016). Qrev—software for computation and quality assurance of acoustic doppler current profiler moving-boat streamflow measurements—user’s manual. Rapport technique, US Geological Survey.
- MUSTE, M., LEE, K. et BERTRAND-KRAJEWSKI, J.-L. (2012). Standardized uncertainty analysis for hydrometry: a review of relevant approaches and implementation examples. *Hydrological Sciences Journal*, 57(4):643–667.
- OBERG, K. et MUELLER, D. S. (2007). Validation of streamflow measurements made with acoustic Doppler current profilers. *Journal of Hydraulic Engineering*, 133(12):1421–1432.
- PIERREFEU, G., BERTHET, T., LE BOURSICAUD, R., BOMPART, P., TRIOL, T. et BLANQUART, B. (2017). OURSIN : OUtil de Répartition deS INcertitudes de mesure de débit par ADCP mobile. *SHF, Colloque Hydrométrie 2017, Lyon*. 17 p.
- POBANZ, K., LE COZ, J., HAUET, A., T., F., LONGEFAY, Y. et PIERREFEU, G. (2015). Intercomparaison ADCP/SVR sur le Rhône à l’aval du barrage de Génissiat, 25 au 28 septembre 2012. Rapport d’essais, Groupe Doppler Hydrométrie. 40 p.
- POBANZ, K., LE COZ, J. et PIERREFEU, G. (2011). Intercomparaison ADCP sur le Rhône à l’aval du barrage de Génissiat (12-15/10/2010). Rapport d’essais, Groupe Doppler. 59 p.
- TEREK, B. et NIMAC, N. (2008). Interkomparacijsko mjerjenje protoka akustickim Doppler (ADCP) protokomjerima. Rapport d’essais.

#### ACKNOWLEDGEMENT

*We thank all the participants, from France and foreign countries, for their mobilization during this event. We thank all the coordinating team, EDF-DTG staff for their help to install and prepare the site and we grateful thank Alexandre Hauet, "orchestra conductor", for the flawless organization of this event. We also thank the dam operator that enable us to perform these experiments. This study is financed by SCHAPI (SRNH 2016 and 2017 conventions) and EDF-DTG. The authors would also like to thank our collaborators at the United States Geological Survey - Office of Surface Water for ongoing discussions and collaborations. Lastly we thank the Groupe Doppler Hydrométrie for discussions and for gathering ADCP users.*